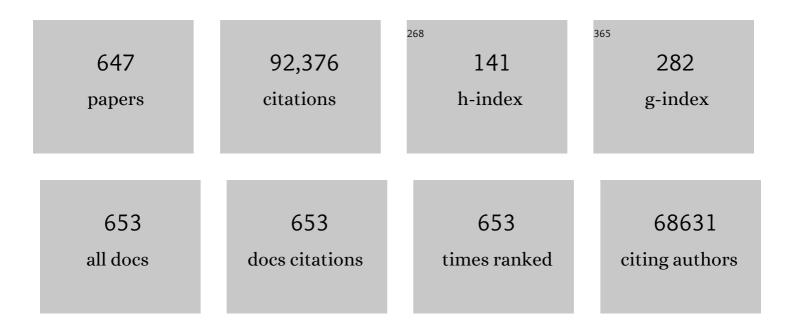
## William A Goddard

List of Publications by Year in descending order

Source: https://exaly.com/author-pdf/10627590/publications.pdf Version: 2024-02-01



#	Article	IF	CITATIONS
1	DREIDING: a generic force field for molecular simulations. The Journal of Physical Chemistry, 1990, 94, 8897-8909.	2.9	5,555
2	ReaxFF:Â A Reactive Force Field for Hydrocarbons. Journal of Physical Chemistry A, 2001, 105, 9396-9409.	2.5	4,490
3	Starburst Dendrimers: Molecular-Level Control of Size, Shape, Surface Chemistry, Topology, and Flexibility from Atoms to Macroscopic Matter. Angewandte Chemie International Edition in English, 1990, 29, 138-175.	4.4	3,032
4	Charge equilibration for molecular dynamics simulations. The Journal of Physical Chemistry, 1991, 95, 3358-3363.	2.9	2,910
5	Advances in molecular quantum chemistry contained in the Q-Chem 4 program package. Molecular Physics, 2015, 113, 184-215.	1.7	2,561
6	Silicon nanowires as efficient thermoelectric materials. Nature, 2008, 451, 168-171.	27.8	2,493
7	ReaxFF Reactive Force Field for Molecular Dynamics Simulations of Hydrocarbon Oxidation. Journal of Physical Chemistry A, 2008, 112, 1040-1053.	2.5	1,892
8	Catalysis Research of Relevance to Carbon Management:  Progress, Challenges, and Opportunities. Chemical Reviews, 2001, 101, 953-996.	47.7	1,311
9	Ultrafine jagged platinum nanowires enable ultrahigh mass activity for the oxygen reduction reaction. Science, 2016, 354, 1414-1419.	12.6	1,292
10	Accurate First Principles Calculation of Molecular Charge Distributions and Solvation Energies from Ab Initio Quantum Mechanics and Continuum Dielectric Theory. Journal of the American Chemical Society, 1994, 116, 11875-11882.	13.7	1,026
11	Thermal conductivity of carbon nanotubes. Nanotechnology, 2000, 11, 65-69.	2.6	988
12	From The Cover: The X3LYP extended density functional for accurate descriptions of nonbond interactions, spin states, and thermochemical properties. Proceedings of the National Academy of Sciences of the United States of America, 2004, 101, 2673-2677.	7.1	863
13	ReaxFFSiO Reactive Force Field for Silicon and Silicon Oxide Systems. Journal of Physical Chemistry A, 2003, 107, 3803-3811.	2.5	821
14	Covalent Organic Frameworks as Exceptional Hydrogen Storage Materials. Journal of the American Chemical Society, 2008, 130, 11580-11581.	13.7	746
15	Linear Artificial Molecular Muscles. Journal of the American Chemical Society, 2005, 127, 9745-9759.	13.7	660
16	Theoretical predictions for hot-carrier generation from surface plasmon decay. Nature Communications, 2014, 5, 5788.	12.8	600
17	Field-effect transistors made from solution-grown two-dimensional tellurene. Nature Electronics, 2018, 1, 228-236.	26.0	591
18	Predictions of Hole Mobilities in Oligoacene Organic Semiconductors from Quantum Mechanical Calculationsâ€. Journal of Physical Chemistry B, 2004, 108, 8614-8621.	2.6	586

#	Article	IF	CITATIONS
19	Excited States of H2O using improved virtual orbitals. Chemical Physics Letters, 1969, 3, 414-418.	2.6	579
20	Calculation of Solvation Free Energies of Charged Solutes Using Mixed Cluster/Continuum Models. Journal of Physical Chemistry B, 2008, 112, 9709-9719.	2.6	567
21	Self-assembly of carbon nanotubes into two-dimensional geometries using DNA origami templates. Nature Nanotechnology, 2010, 5, 61-66.	31.5	567
22	Temperature Dependence of Blue Phosphorescent Cyclometalated Ir(III) Complexes. Journal of the American Chemical Society, 2009, 131, 9813-9822.	13.7	558
23	Recent advances on simulation and theory of hydrogen storage in metal–organic frameworks and covalent organic frameworks. Chemical Society Reviews, 2009, 38, 1460.	38.1	535
24	Nonradiative Plasmon Decay and Hot Carrier Dynamics: Effects of Phonons, Surfaces, and Geometry. ACS Nano, 2016, 10, 957-966.	14.6	534
25	Phosphofructokinase 1 Glycosylation Regulates Cell Growth and Metabolism. Science, 2012, 337, 975-980.	12.6	527
26	Software for the frontiers of quantum chemistry: An overview of developments in the Q-Chem 5 package. Journal of Chemical Physics, 2021, 155, 084801.	3.0	518
27	Starburst dendrimers. 5. Molecular shape control. Journal of the American Chemical Society, 1989, 111, 2339-2341.	13.7	500
28	Shock Waves in High-Energy Materials: The Initial Chemical Events in Nitramine RDX. Physical Review Letters, 2003, 91, 098301.	7.8	495
29	Sulfation patterns of glycosaminoglycans encode molecular recognition and activity. Nature Chemical Biology, 2006, 2, 467-473.	8.0	494
30	Oxidative Aliphatic C-H Fluorination with Fluoride Ion Catalyzed by a Manganese Porphyrin. Science, 2012, 337, 1322-1325.	12.6	478
31	Starburstâ€Dendrimere: Kontrolle von Größe, Gestalt, OberflÜhenchemie, Topologie und Flexibilitä beim Übergang von Atomen zu makroskopischer Materie. Angewandte Chemie, 1990, 102, 119-157.	2.0	473
32	Generalized valence bond description of bonding in low-lying states of molecules. Accounts of Chemical Research, 1973, 6, 368-376.	15.6	467
33	Single-atom tailoring of platinum nanocatalysts for high-performance multifunctional electrocatalysis. Nature Catalysis, 2019, 2, 495-503.	34.4	464
34	Origin of low sodium capacity in graphite and generally weak substrate binding of Na and Mg among alkali and alkaline earth metals. Proceedings of the National Academy of Sciences of the United States of America, 2016, 113, 3735-3739.	7.1	462
35	Structure of PAMAM Dendrimers:Â Generations 1 through 11. Macromolecules, 2004, 37, 6236-6254.	4.8	455
36	A bonding model for gold(I) carbene complexes. Nature Chemistry, 2009, 1, 482-486.	13.6	451

#	Article	IF	CITATIONS
37	Energetics, structure, mechanical and vibrational properties of single-walled carbon nanotubes. Nanotechnology, 1998, 9, 184-191.	2.6	448
38	Accurate Band Gaps for Semiconductors from Density Functional Theory. Journal of Physical Chemistry Letters, 2011, 2, 212-217.	4.6	444
39	Schottky-Barrier-Free Contacts with Two-Dimensional Semiconductors by Surface-Engineered MXenes. Journal of the American Chemical Society, 2016, 138, 15853-15856.	13.7	444
40	Mechanically bonded macromolecules. Chemical Society Reviews, 2010, 39, 17-29.	38.1	428
41	The two-phase model for calculating thermodynamic properties of liquids from molecular dynamics: Validation for the phase diagram of Lennard-Jones fluids. Journal of Chemical Physics, 2003, 119, 11792-11805.	3.0	426
42	Nanophase-Segregation and Transport in Nafion 117 from Molecular Dynamics Simulations:Â Effect of Monomeric Sequence. Journal of Physical Chemistry B, 2004, 108, 3149-3157.	2.6	425
43	Lithium-Doped Metal-Organic Frameworks for Reversible H <sub>2</sub> Storage at Ambient Temperature. Journal of the American Chemical Society, 2007, 129, 8422-8423.	13.7	418
44	Full atomistic reaction mechanism with kinetics for CO reduction on Cu(100) from ab initio molecular dynamics free-energy calculations at 298 K. Proceedings of the National Academy of Sciences of the United States of America, 2017, 114, 1795-1800.	7.1	414
45	Acceleration of convergence for lattice sums. The Journal of Physical Chemistry, 1989, 93, 7320-7327.	2.9	405
46	Atomic level simulations on a million particles: The cell multipole method for Coulomb and London nonbond interactions. Journal of Chemical Physics, 1992, 97, 4309-4315.	3.0	404
47	ReaxFF- <i>l</i> g: Correction of the ReaxFF Reactive Force Field for London Dispersion, with Applications to the Equations of State for Energetic Materials. Journal of Physical Chemistry A, 2011, 115, 11016-11022.	2.5	401
48	Oxidation of Methanol on 2nd and 3rd Row Group VIII Transition Metals (Pt, Ir, Os, Pd, Rh, and Ru): Application to Direct Methanol Fuel Cells. Journal of the American Chemical Society, 1999, 121, 10928-10941.	13.7	397
49	Simulations on the Thermal Decomposition of a Poly(dimethylsiloxane) Polymer Using the ReaxFF Reactive Force Field. Journal of the American Chemical Society, 2005, 127, 7192-7202.	13.7	395
50	Oxygenâ€Vacancy Abundant Ultrafine Co <sub>3</sub> O <sub>4</sub> /Graphene Composites for Highâ€Rate Supercapacitor Electrodes. Advanced Science, 2018, 5, 1700659.	11.2	392
51	Development of the ReaxFF Reactive Force Field for Describing Transition Metal Catalyzed Reactions, with Application to the Initial Stages of the Catalytic Formation of Carbon Nanotubes. Journal of Physical Chemistry A, 2005, 109, 493-499.	2.5	390
52	Effect of Solvent and pH on the Structure of PAMAM Dendrimers. Macromolecules, 2005, 38, 979-991.	4.8	389
53	Synergy between Fe and Ni in the optimal performance of (Ni,Fe)OOH catalysts for the oxygen evolution reaction. Proceedings of the National Academy of Sciences of the United States of America, 2018, 115, 5872-5877.	7.1	380
54	Thermal decomposition of RDX from reactive molecular dynamics. Journal of Chemical Physics, 2005, 122, 054502.	3.0	366

#	Article	IF	CITATIONS
55	Subsurface oxide plays a critical role in CO <sub>2</sub> activation by Cu(111) surfaces to form chemisorbed CO <sub>2</sub> , the first step in reduction of CO <sub>2</sub> . Proceedings of the National Academy of Sciences of the United States of America, 2017, 114, 6706-6711.	7.1	363
56	Melting and crystallization in Ni nanoclusters: The mesoscale regime. Journal of Chemical Physics, 2001, 115, 385-394.	3.0	345
57	Doubly hybrid density functional for accurate descriptions of nonbond interactions, thermochemistry, and thermochemical kinetics. Proceedings of the National Academy of Sciences of the United States of America, 2009, 106, 4963-4968.	7.1	332
58	Evaluation of B3LYP, X3LYP, and M06-Class Density Functionals for Predicting the Binding Energies of Neutral, Protonated, and Deprotonated Water Clusters. Journal of Chemical Theory and Computation, 2009, 5, 1016-1026.	5.3	326
59	Monolayer atomic crystal molecular superlattices. Nature, 2018, 555, 231-236.	27.8	323
60	Prediction of fullerene packing in C60 and C70 crystals. Nature, 1991, 351, 464-467.	27.8	312
61	Efficient hydrogen evolution by ternary molybdenum sulfoselenide particles on self-standing porous nickel diselenide foam. Nature Communications, 2016, 7, 12765.	12.8	312
62	Thermal conductivity of diamond and related materials from molecular dynamics simulations. Journal of Chemical Physics, 2000, 113, 6888-6900.	3.0	307
63	New Alkali Doped Pillared Carbon Materials Designed to Achieve Practical Reversible Hydrogen Storage for Transportation. Physical Review Letters, 2004, 92, 166103.	7.8	307
64	Toward a Lithium–"Air―Battery: The Effect of CO <sub>2</sub> on the Chemistry of a Lithium–Oxygen Cell. Journal of the American Chemical Society, 2013, 135, 9733-9742.	13.7	307
65	Highly active and stable stepped Cu surface for enhanced electrochemical CO2 reduction to C2H4. Nature Catalysis, 2020, 3, 804-812.	34.4	298
66	First-Principles Investigation of Anistropic Hole Mobilities in Organic Semiconductors. Journal of Physical Chemistry B, 2009, 113, 8813-8819.	2.6	292
67	Development and Validation of ReaxFF Reactive Force Field for Hydrocarbon Chemistry Catalyzed by Nickel. Journal of Physical Chemistry C, 2010, 114, 4939-4949.	3.1	288
68	Entropy and the driving force for the filling of carbon nanotubes with water. Proceedings of the National Academy of Sciences of the United States of America, 2011, 108, 11794-11798.	7.1	287
69	Radically enhanced molecular recognition. Nature Chemistry, 2010, 2, 42-49.	13.6	280
70	Two-Phase Thermodynamic Model for Efficient and Accurate Absolute Entropy of Water from Molecular Dynamics Simulations. Journal of Physical Chemistry B, 2010, 114, 8191-8198.	2.6	277
71	Prediction of structure and function of G protein-coupled receptors. Proceedings of the National Academy of Sciences of the United States of America, 2002, 99, 12622-12627.	7.1	276
72	In Silico Discovery of New Dopants for Fe-Doped Ni Oxyhydroxide (Ni <sub>1–<i>x</i></sub> Fe <sub><i>x</i></sub> OOH) Catalysts for Oxygen Evolution Reaction. Journal of the American Chemical Society, 2018, 140, 6745-6748.	13.7	274

#	Article	IF	CITATIONS
73	Mechanism of Câ^'F Reductive Elimination from Palladium(IV) Fluorides. Journal of the American Chemical Society, 2010, 132, 3793-3807.	13.7	273
74	Dendrimer Enhanced Ultrafiltration. 1. Recovery of Cu(II) from Aqueous Solutions Using PAMAM Dendrimers with Ethylene Diamine Core and Terminal NH2Groups. Environmental Science & Technology, 2005, 39, 1366-1377.	10.0	272
75	Improved Quantum Theory of Many-Electron Systems. II. The Basic Method. Physical Review, 1967, 157, 81-93.	2.7	269
76	Strain Rate Induced Amorphization in Metallic Nanowires. Physical Review Letters, 1999, 82, 2900-2903.	7.8	268
77	Source of Image Contrast in STM Images of Functionalized Alkanes on Graphite:Â A Systematic Functional Group Approach. Journal of Physical Chemistry B, 1997, 101, 5978-5995.	2.6	267
78	New surfactant classes for enhanced oil recovery and their tertiary oil recovery potential. Journal of Petroleum Science and Engineering, 2010, 71, 23-29.	4.2	264
79	Electronicâ^'Mechanical Coupling in Graphene from in situ Nanoindentation Experiments and Multiscale Atomistic Simulations. Nano Letters, 2011, 11, 1241-1246.	9.1	261
80	Carbon Cluster Formation during Thermal Decomposition of Octahydro-1,3,5,7-tetranitro-1,3,5,7-tetrazocine and 1,3,5-Triamino-2,4,6-trinitrobenzene High Explosives from ReaxFF Reactive Molecular Dynamics Simulations. Journal of Physical Chemistry A, 2009, 113, 10619-10640.	2.5	257
81	Antibody Catalysis of the Oxidation of Water. Science, 2001, 293, 1806-1811.	12.6	254
82	Ab initiostudies of the x-ray absorption edge in copper complexes. I. AtomicCu2+and Cu(ii)Cl2. Physical Review B, 1980, 22, 2767-2776.	3.2	252
83	Molecular-dynamics simulations of glass formation and crystallization in binary liquid metals: Cu-Ag and Cu-Ni. Physical Review B, 1999, 59, 3527-3533.	3.2	252
84	Olefin metathesis - a mechanistic study of high-valent Group VI catalysts. Journal of the American Chemical Society, 1982, 104, 448-456.	13.7	251
85	PAMAM Dendrimers Undergo pH Responsive Conformational Changes without Swelling. Journal of the American Chemical Society, 2009, 131, 2798-2799.	13.7	249
86	Molecular Dynamics Study of a Surfactant-Mediated Decaneâ^'Water Interface:  Effect of Molecular Architecture of Alkyl Benzene Sulfonate. Journal of Physical Chemistry B, 2004, 108, 12130-12140.	2.6	244
87	The Mechanism for Unimolecular Decomposition of RDX (1,3,5-Trinitro-1,3,5-triazine), an ab Initio Study. Journal of Physical Chemistry A, 2000, 104, 2261-2272.	2.5	241
88	Bimetallic Reductive Elimination from Dinuclear Pd(III) Complexes. Journal of the American Chemical Society, 2010, 132, 14092-14103.	13.7	237
89	ReaxFFMgHReactive Force Field for Magnesium Hydride Systems. Journal of Physical Chemistry A, 2005, 109, 851-859.	2.5	234
90	Theoretical studies of oxidative addition and reductive elimination. 2. Reductive coupling of hydrogen-hydrogen, hydrogen-carbon, and carbon-carbon bonds from palladium and platinum complexes. Organometallics, 1986, 5, 609-622.	2.3	228

#	Article	IF	CITATIONS
91	Molecular dynamics study of the binaryCu46Zr54metallic glass motivated by experiments: Glass formation and atomic-level structure. Physical Review B, 2005, 71, .	3.2	227
92	Self-Assembled Monolayer Mechanism for Corrosion Inhibition of Iron by Imidazolines. Langmuir, 1996, 12, 6419-6428.	3.5	225
93	Formation of carbon–nitrogen bonds in carbon monoxide electrolysis. Nature Chemistry, 2019, 11, 846-851.	13.6	223
94	Improved Quantum Theory of Many-Electron Systems. I. Construction of Eigenfunctions ofS^2Which Satisfy Pauli's Principle. Physical Review, 1967, 157, 73-80.	2.7	222
95	Configuration interaction studies of O3 and O+3. Ground and excited states. Journal of Chemical Physics, 1975, 62, 3912-3924.	3.0	221
96	Multiparadigm Modeling of Dynamical Crack Propagation in Silicon Using a Reactive Force Field. Physical Review Letters, 2006, 96, 095505.	7.8	214
97	Initiation Mechanisms and Kinetics of Pyrolysis and Combustion of JP-10 Hydrocarbon Jet Fuel. Journal of Physical Chemistry A, 2009, 113, 1740-1746.	2.5	213
98	Improved Designs of Metal–Organic Frameworks for Hydrogen Storage. Angewandte Chemie - International Edition, 2007, 46, 6289-6292.	13.8	212
99	Phosphoramidite Gold(I)-Catalyzed Diastereo- and Enantioselective Synthesis of 3,4-Substituted Pyrrolidines. Journal of the American Chemical Society, 2011, 133, 5500-5507.	13.7	210
100	Improved Quantum Theory of Many lectron Systems. V. The Spinâ€Coupling Optimized GI Method. Journal of Chemical Physics, 1969, 51, 1073-1087.	3.0	207
101	Free-Energy Barriers and Reaction Mechanisms for the Electrochemical Reduction of CO on the Cu(100) Surface, Including Multiple Layers of Explicit Solvent at pH 0. Journal of Physical Chemistry Letters, 2015, 6, 4767-4773.	4.6	206
102	Stabilizing Highly Active Ru Sites by Suppressing Lattice Oxygen Participation in Acidic Water Oxidation. Journal of the American Chemical Society, 2021, 143, 6482-6490.	13.7	204
103	Dendritic Chelating Agents. 1. Cu(II) Binding to Ethylene Diamine Core Poly(amidoamine) Dendrimers in Aqueous Solutions. Langmuir, 2004, 20, 2640-2651.	3.5	200
104	Resolution of the Band Gap Prediction Problem for Materials Design. Journal of Physical Chemistry Letters, 2016, 7, 1198-1203.	4.6	200
105	Poly(amidoamine) Dendrimers:  A New Class of High Capacity Chelating Agents for Cu(II) Ions. Environmental Science & Technology, 1999, 33, 820-824.	10.0	198
106	Theoretical Study of Solvent Effects on the Platinum-Catalyzed Oxygen Reduction Reaction. Journal of Physical Chemistry Letters, 2010, 1, 856-861.	4.6	195
107	pKaValues of Guanine in Water:Â Density Functional Theory Calculations Combined with Poissonâ~'Boltzmann Continuumâ~'Solvation Model. Journal of Physical Chemistry B, 2003, 107, 344-357.	2.6	193
108	The Self-Consistent Field Equations for Generalized Valence Bond and Open-Shell Hartree—Fock Wave Functions. , 1977, , 79-127.		193

#	Article	IF	CITATIONS
109	Ultrahigh Mass Activity for Carbon Dioxide Reduction Enabled by Gold–Iron Core–Shell Nanoparticles. Journal of the American Chemical Society, 2017, 139, 15608-15611.	13.7	191
110	Oxygen evolution reaction over catalytic single-site Co in a well-defined brookite TiO2 nanorod surface. Nature Catalysis, 2021, 4, 36-45.	34.4	189
111	Defect-enriched iron fluoride-oxide nanoporous thin films bifunctional catalyst for water splitting. Nature Communications, 2018, 9, 1809.	12.8	188
112	First Principles Calculation of pKa Values for 5-Substituted Uracils. Journal of Physical Chemistry A, 2001, 105, 274-280.	2.5	185
113	Adhesion and nonwetting-wetting transition in the Al/Î $\pm$ â $^{3}$ Al2O3interface. Physical Review B, 2004, 69, .	3.2	184
114	Mechanism of Homogeneous Ir(III) Catalyzed Regioselective Arylation of Olefins. Journal of the American Chemical Society, 2004, 126, 352-363.	13.7	184
115	Early maturation processes in coal. Part 2: Reactive dynamics simulations using the ReaxFF reactive force field on Morwell Brown coal structures. Organic Geochemistry, 2009, 40, 1195-1209.	1.8	183
116	Antiferromagnetic band structure ofLa2CuO4: Becke-3–Lee-Yang-Parr calculations. Physical Review B, 2001, 63, .	3.2	182
117	Development of a ReaxFF Reactive Force Field for Glycine and Application to Solvent Effect and Tautomerization. Journal of Physical Chemistry B, 2011, 115, 249-261.	2.6	182
118	Definitive Band Gaps for Single-Wall Carbon Nanotubes. Journal of Physical Chemistry Letters, 2010, 1, 2946-2950.	4.6	179
119	Outstanding hydrogen evolution reaction catalyzed by porous nickel diselenide electrocatalysts. Energy and Environmental Science, 2017, 10, 1487-1492.	30.8	176
120	Bonding Properties of the Water Dimer:Â A Comparative Study of Density Functional Theories. Journal of Physical Chemistry A, 2004, 108, 2305-2313.	2.5	174
121	Alkylgold complexes by the intramolecular aminoauration of unactivated alkenes. Chemical Science, 2010, 1, 226.	7.4	174
122	Morse Stretch Potential Charge Equilibrium Force Field for Ceramics: Application to the Quartz-Stishovite Phase Transition and to Silica Glass. Physical Review Letters, 1999, 82, 1708-1711.	7.8	173
123	The Reaction Mechanism with Free Energy Barriers for Electrochemical Dihydrogen Evolution on MoS <sub>2</sub> . Journal of the American Chemical Society, 2015, 137, 6692-6698.	13.7	173
124	Effects of Surface Roughness on the Electrochemical Reduction of CO <sub>2</sub> over Cu. ACS Energy Letters, 2020, 5, 1206-1214.	17.4	172
125	Highly stable tetrathiafulvalene radical dimers in [3]catenanes. Nature Chemistry, 2010, 2, 870-879.	13.6	171
126	Metalâ^'Organic Frameworks Provide Large Negative Thermal Expansion Behavior. Journal of Physical Chemistry C, 2007, 111, 15185-15191.	3.1	170

#	Article	IF	CITATIONS
127	Electrochemical CO Reduction Builds Solvent Water into Oxygenate Products. Journal of the American Chemical Society, 2018, 140, 9337-9340.	13.7	170
128	The charge-asymmetric nonlocally determined local-electric (CANDLE) solvation model. Journal of Chemical Physics, 2015, 142, 064107.	3.0	167
129	Stabilization of Coiled-Coil Peptide Domains by Introduction of Trifluoroleucineâ€. Biochemistry, 2001, 40, 2790-2796.	2.5	166
130	BrÃ,nsted basicity of the air–water interface. Proceedings of the National Academy of Sciences of the United States of America, 2012, 109, 18679-18683.	7.1	159
131	A Radically Configurable Six-State Compound. Science, 2013, 339, 429-433.	12.6	158
132	The predicted 3D structure of the human D2 dopamine receptor and the binding site and binding affinities for agonists and antagonists. Proceedings of the National Academy of Sciences of the United States of America, 2004, 101, 3815-3820.	7.1	157
133	Pressureâ€Dependent Polymorphism and Bandâ€Gap Tuning of Methylammonium Lead Iodide Perovskite. Angewandte Chemie - International Edition, 2016, 55, 6540-6544.	13.8	157
134	Development and Validation of a ReaxFF Reactive Force Field for Cu Cation/Water Interactions and Copper Metal/Metal Oxide/Metal Hydroxide Condensed Phases. Journal of Physical Chemistry A, 2010, 114, 9507-9514.	2.5	156
135	Mechanical properties and force field parameters for polyethylene crystal. The Journal of Physical Chemistry, 1991, 95, 2260-2272.	2.9	154
136	On the Impact of Steric and Electronic Properties of Ligands on Gold(I)-Catalyzed Cycloaddition Reactions. Organic Letters, 2009, 11, 4798-4801.	4.6	153
137	The extended Perdew-Burke-Ernzerhof functional with improved accuracy for thermodynamic and electronic properties of molecular systems. Journal of Chemical Physics, 2004, 121, 4068-4082.	3.0	150
138	Computational and experimental demonstrations of one-pot tandem catalysis for electrochemical carbon dioxide reduction to methane. Nature Communications, 2019, 10, 3340.	12.8	150
139	Atomistic-Scale Simulations of the Initial Chemical Events in the Thermal Initiation of Triacetonetriperoxide. Journal of the American Chemical Society, 2005, 127, 11053-11062.	13.7	147
140	Application of the ReaxFF Reactive Force Field to Reactive Dynamics of Hydrocarbon Chemisorption and Decomposition. Journal of Physical Chemistry C, 2010, 114, 5675-5685.	3.1	147
141	Mechanistic Analysis of Hydroarylation Catalysts. Journal of the American Chemical Society, 2004, 126, 11658-11665.	13.7	146
142	Alkyl polyglycoside surfactant–alcohol cosolvent formulations for improved oil recovery. Colloids and Surfaces A: Physicochemical and Engineering Aspects, 2009, 339, 48-59.	4.7	146
143	Nature of the Active Sites for CO Reduction on Copper Nanoparticles; Suggestions for Optimizing Performance. Journal of the American Chemical Society, 2017, 139, 11642-11645.	13.7	146
144	Thermodynamics of liquids: standard molar entropies and heat capacities of common solvents from 2PT molecular dynamics. Physical Chemistry Chemical Physics, 2011, 13, 169-181.	2.8	144

#	Article	IF	CITATIONS
145	A fast doubly hybrid density functional method close to chemical accuracy using a local opposite spin ansatz. Proceedings of the National Academy of Sciences of the United States of America, 2011, 108, 19896-19900.	7.1	143
146	Mechanical and Transport Properties of the Poly(ethylene oxide)â^'Poly(acrylic acid) Double Network Hydrogel from Molecular Dynamic Simulations. Journal of Physical Chemistry B, 2007, 111, 1729-1737.	2.6	142
147	Reaction mechanism and kinetics for CO2 reduction on nickel single atom catalysts from quantum mechanics. Nature Communications, 2020, 11, 2256.	12.8	140
148	Flexible d basis sets for scandium through copper. The Journal of Physical Chemistry, 1981, 85, 2607-2611.	2.9	139
149	Development and Application of a ReaxFF Reactive Force Field for Oxidative Dehydrogenation on Vanadium Oxide Catalysts. Journal of Physical Chemistry C, 2008, 112, 14645-14654.	3.1	138
150	Water adsorption on stepped ZnO surfaces from MD simulation. Surface Science, 2010, 604, 741-752.	1.9	138
151	Ab InitioEffective Potentials for Use in Molecular Calculations. Journal of Chemical Physics, 1972, 56, 2685-2701.	3.0	134
152	Accurate Energies and Structures for Large Water Clusters Using the X3LYP Hybrid Density Functional. Journal of Physical Chemistry A, 2004, 108, 10518-10526.	2.5	134
153	A Highly Active Star Decahedron Cu Nanocatalyst for Hydrocarbon Production at Low Overpotentials. Advanced Materials, 2019, 31, e1805405.	21.0	134
154	Electrocatalysis at Organic–Metal Interfaces: Identification of Structure–Reactivity Relationships for CO <sub>2</sub> Reduction at Modified Cu Surfaces. Journal of the American Chemical Society, 2019, 141, 7355-7364.	13.7	133
155	Dynamics and Thermodynamics of Water in PAMAM Dendrimers at Subnanosecond Time Scales. Journal of Physical Chemistry B, 2005, 109, 8663-8672.	2.6	131
156	pKa Calculations of Aliphatic Amines, Diamines, and Aminoamides via Density Functional Theory with a Poissonâ^'Boltzmann Continuum Solvent Model. Journal of Physical Chemistry A, 2007, 111, 4422-4430.	2.5	131
157	New pseudospectral algorithms for electronic structure calculations: Length scale separation and analytical twoâ€electron integral corrections. Journal of Chemical Physics, 1994, 101, 4028-4041.	3.0	129
158	Dynamic Transition in the Structure of an Energetic Crystal during Chemical Reactions at Shock Front Prior to Detonation. Physical Review Letters, 2007, 99, 148303.	7.8	129
159	The Inner-Sphere Process in the Enantioselective Tsuji Allylation Reaction with ( <i>S</i> )- <i>t</i> -Bu-phosphinooxazoline Ligands. Journal of the American Chemical Society, 2007, 129, 11876-11877.	13.7	129
160	Density-Dependent Liquid Nitromethane Decomposition: Molecular Dynamics Simulations Based on ReaxFF. Journal of Physical Chemistry A, 2011, 115, 10181-10202.	2.5	129
161	Decomposition of Condensed Phase Energetic Materials: Interplay between Uni- and Bimolecular Mechanisms. Journal of the American Chemical Society, 2014, 136, 4192-4200.	13.7	126
162	Reaction Mechanism and Kinetics for Ammonia Synthesis on the Fe(111) Surface. Journal of the American Chemical Society, 2018, 140, 6288-6297.	13.7	126

#	Article	IF	CITATIONS
163	Modified Generalized Valence-Bond Method: A Simple Correction for the Electron Correlation Missing in Generalized Valence-Bond Wave Functions; Prediction of Double-Well States forCr2andMo2. Physical Review Letters, 1985, 54, 661-664.	7.8	124
164	Product Protection, the Key to Developing High Performance Methane Selective Oxidation Catalysts. Journal of the American Chemical Society, 2009, 131, 17110-17115.	13.7	124
165	<i>Ab initio</i> phonon coupling and optical response of hot electrons in plasmonic metals. Physical Review B, 2016, 94, .	3.2	124
166	Atomistic Description of Ionic Diffusion in PEO–LiTFSI: Effect of Temperature, Molecular Weight, and Ionic Concentration. Macromolecules, 2018, 51, 8987-8995.	4.8	124
167	Solution-Phase Mechanistic Study and Solid-State Structure of a Tris(bipyridinium radical cation) Inclusion Complex. Journal of the American Chemical Society, 2012, 134, 3061-3072.	13.7	123
168	Predicted 3D structure for the human Â2 adrenergic receptor and its binding site for agonists and antagonists. Proceedings of the National Academy of Sciences of the United States of America, 2004, 101, 2736-2741.	7.1	122
169	Stability and Thermodynamics of the PtCl2Type Catalyst for Activating Methane to Methanol:Â A Computational Study. Organometallics, 2002, 21, 511-525.	2.3	121
170	Threshold Crack Speed Controls Dynamical Fracture of Silicon Single Crystals. Physical Review Letters, 2007, 99, 165502.	7.8	121
171	Energetics of Third-Row Transition Metal Methylidene Ions MCH2+ (M = La, Hf, Ta, W, Re, Os, Ir, Pt, Au). Journal of the American Chemical Society, 1994, 116, 8733-8740.	13.7	119
172	The ferroelectric and cubic phases in BaTiO3 ferroelectrics are also antiferroelectric. Proceedings of the United States of America, 2006, 103, 14695-14700.	7.1	119
173	Calculation of Mechanical, Thermodynamic and Transport Properties of Metallic Glass Formers. Materials Research Society Symposia Proceedings, 1998, 554, 43.	0.1	117
174	Position of K Atoms in Doped Single-Walled Carbon Nanotube Crystals. Physical Review Letters, 1998, 80, 5556-5559.	7.8	117
175	A Two-Stage Mechanism of Bimetallic Catalyzed Growth of Single-Walled Carbon Nanotubes. Nano Letters, 2004, 4, 2331-2335.	9.1	116
176	Dynamics of the Dissociation of Hydrogen on Stepped Platinum Surfaces Using the ReaxFF Reactive Force Field. Journal of Physical Chemistry B, 2006, 110, 4274-4282.	2.6	116
177	Experimental and <i>AbÂlnitio</i> Ultrafast Carrier Dynamics in Plasmonic Nanoparticles. Physical Review Letters, 2017, 118, 087401.	7.8	116
178	Reaction Mechanism for the Hydrogen Evolution Reaction on the Basal Plane Sulfur Vacancy Site of MoS <sub>2</sub> Using Grand Canonical Potential Kinetics. Journal of the American Chemical Society, 2018, 140, 16773-16782.	13.7	116
179	Fractal atomic-level percolation in metallic glasses. Science, 2015, 349, 1306-1310.	12.6	114
180	Relative Unidirectional Translation in an Artificial Molecular Assembly Fueled by Light. Journal of the American Chemical Society, 2013, 135, 18609-18620.	13.7	112

#	Article	IF	CITATIONS
181	Quantum-mechanical calculations of the stabilities of fluxional isomers of C4HFormula in solution. Proceedings of the National Academy of Sciences of the United States of America, 2003, 100, 15-19.	7.1	111
182	M3B:  A Coarse Grain Force Field for Molecular Simulations of Malto-Oligosaccharides and Their Water Mixtures. Journal of Physical Chemistry B, 2004, 108, 1414-1427.	2.6	111
183	A Push-Button Molecular Switch. Journal of the American Chemical Society, 2009, 131, 11571-11580.	13.7	111
184	Substrate assistance in the mechanism of family 18 chitinases: theoretical studies of potential intermediates and inhibitors 1 1Edited by B. Honig. Journal of Molecular Biology, 1998, 280, 913-923.	4.2	110
185	Computational Study of Copper(II) Complexation and Hydrolysis in Aqueous Solutions Using Mixed Cluster/Continuum Models. Journal of Physical Chemistry A, 2009, 113, 9559-9567.	2.5	110
186	Oxygen Hydration Mechanism for the Oxygen Reduction Reaction at Pt and Pd Fuel Cell Catalysts. Journal of Physical Chemistry Letters, 2011, 2, 572-576.	4.6	110
187	Atomistic Origin of Brittle Failure of Boron Carbide from Large-Scale Reactive Dynamics Simulations: Suggestions toward Improved Ductility. Physical Review Letters, 2015, 115, 105501.	7.8	109
188	The Source of Helicity in PerfluorinatedN-Alkanes. Macromolecules, 2003, 36, 5331-5341.	4.8	108
189	Water Formation on Pt and Pt-based Alloys: A Theoretical Description of a Catalytic Reaction. ChemPhysChem, 2006, 7, 992-1005.	2.1	107
190	Simulating the Initial Stage of Phenolic Resin Carbonization via the ReaxFF Reactive Force Field. Journal of Physical Chemistry A, 2009, 113, 6891-6894.	2.5	107
191	General Multiobjective Force Field Optimization Framework, with Application to Reactive Force Fields for Silicon Carbide. Journal of Chemical Theory and Computation, 2014, 10, 1426-1439.	5.3	107
192	Identifying Active Sites for CO <sub>2</sub> Reduction on Dealloyed Gold Surfaces by Combining Machine Learning with Multiscale Simulations. Journal of the American Chemical Society, 2019, 141, 11651-11657.	13.7	107
193	First Principles Calculations of the Tautomers and pKaValues of 8-Oxoguanine:Â Implications for Mutagenicity and Repair. Chemical Research in Toxicology, 2002, 15, 1023-1035.	3.3	106
194	Nature of the excited states ofHe2. Physical Review A, 1975, 12, 1203-1221.	2.5	105
195	New Concepts of Metallic Bonding Based on Valence-Bond Ideas. Physical Review Letters, 1985, 55, 2563-2566.	7.8	105
196	Thermal Decomposition of Condensed-Phase Nitromethane from Molecular Dynamics from ReaxFF Reactive Dynamics. Journal of Physical Chemistry B, 2011, 115, 6534-6540.	2.6	105
197	Selective Extraction of C <sub>70</sub> by a Tetragonal Prismatic Porphyrin Cage. Journal of the American Chemical Society, 2018, 140, 13835-13842.	13.7	105
198	Selective CO <sub>2</sub> Electrochemical Reduction Enabled by a Tricomponent Copolymer Modifier on a Copper Surface. Journal of the American Chemical Society, 2021, 143, 2857-2865.	13.7	104

#	Article	IF	CITATIONS
199	Thermal Decomposition of Hydrazines from Reactive Dynamics Using the ReaxFF Reactive Force Field. Journal of Physical Chemistry B, 2009, 113, 10770-10778.	2.6	103
200	Mechanism and Kinetics for the Initial Steps of Pyrolysis and Combustion of 1,6-Dicyclopropane-2,4-hexyne from ReaxFF Reactive Dynamics. Journal of Physical Chemistry A, 2011, 115, 4941-4950.	2.5	103
201	The Reaction Mechanism of the Enantioselective Tsuji Allylation: Inner-Sphere and Outer-Sphere Pathways, Internal Rearrangements, and Asymmetric C–C Bond Formation. Journal of the American Chemical Society, 2012, 134, 19050-19060.	13.7	103
202	Improved Quantum Theory of Manyâ€Electron Systems. III. The GF Method. Journal of Chemical Physics, 1968, 48, 450-461.	3.0	102
203	Electrophilic, Ambiphilic, and Nucleophilic Câ^'H Bond Activation: Understanding the Electronic Continuum of Câ^'H Bond Activation Through Transition-State and Reaction Pathway Interaction Energy Decompositions. Organometallics, 2010, 29, 6459-6472.	2.3	102
204	Tellurium: Fast Electrical and Atomic Transport along the Weak Interaction Direction. Journal of the American Chemical Society, 2018, 140, 550-553.	13.7	101
205	Thermal decomposition process in algaenan of Botryococcus braunii race L. Part 2: Molecular dynamics simulations using the ReaxFF reactive force field. Organic Geochemistry, 2009, 40, 416-427.	1.8	100
206	Chemisorption of Organics on Platinum. 2. Chemisorption of C2Hxand CHxon Pt(111). Journal of Physical Chemistry B, 1998, 102, 9492-9500.	2.6	98
207	The Isomerization Equilibrium between Cis and Trans Chloride Ruthenium Olefin Metathesis Catalysts from Quantum Mechanics Calculations. Journal of the American Chemical Society, 2005, 127, 12218-12219.	13.7	98
208	Development of the ReaxFF reactive force field for mechanistic studies of catalytic selective oxidation processes on BiMoO x. Topics in Catalysis, 2006, 38, 93.	2.8	98
209	Elucidating glycosaminoglycan–protein–protein interactions using carbohydrate microarray and computational approaches. Proceedings of the National Academy of Sciences of the United States of America, 2011, 108, 9747-9752.	7.1	98
210	Csp <sup>3</sup> –Csp <sup>3</sup> Bond-Forming Reductive Elimination from Well-Defined Copper(III) Complexes. Journal of the American Chemical Society, 2019, 141, 3153-3159.	13.7	98
211	Distance Dependent Hydrogen Bond Potentials for Nucleic Acid Base Pairs from ab Initio Quantum Mechanical Calculations (LMP2/cc-pVTZ). Journal of Physical Chemistry B, 1997, 101, 4851-4859.	2.6	97
212	Pd-Mediated Activation of Molecular Oxygen in a Nonpolar Medium. Journal of the American Chemical Society, 2005, 127, 13172-13179.	13.7	97
213	Physical mechanism of anisotropic sensitivity in pentaerythritol tetranitrate from compressive-shear reaction dynamics simulations. Applied Physics Letters, 2010, 96, .	3.3	97
214	Protein Dynamics in a Family of Laboratory Evolved Thermophilic Enzymes. Journal of Molecular Biology, 2003, 327, 745-757.	4.2	96
215	First Principles Predictions of the Structure and Function of G-Protein-Coupled Receptors: Validation for Bovine Rhodopsin. Biophysical Journal, 2004, 86, 1904-1921.	0.5	96
216	Hydration of Copper(II): New Insights from Density Functional Theory and the COSMO Solvation Model. Journal of Physical Chemistry A, 2008, 112, 9104-9112.	2.5	96

#	Article	IF	CITATIONS
217	Correlation onsistent configuration interaction: Accurate bond dissociation energies from simple wave functions. Journal of Chemical Physics, 1988, 88, 3132-3140.	3.0	95
218	ReaxFF Reactive Force Field for the Y-Doped BaZrO <sub>3</sub> Proton Conductor with Applications to Diffusion Rates for Multigranular Systems. Journal of Physical Chemistry A, 2008, 112, 11414-11422.	2.5	95
219	A Covalent Organic Framework that Exceeds the DOE 2015 Volumetric Target for H <sub>2</sub> Uptake at 298 K. Journal of Physical Chemistry Letters, 2012, 3, 2671-2675.	4.6	95
220	The gas phase reaction of singlet dioxygen with water: A water-catalyzed mechanism. Proceedings of the United States of America, 2002, 99, 3376-3381.	7.1	94
221	A divide-and-conquer/cellular-decomposition framework for million-to-billion atom simulations of chemical reactions. Computational Materials Science, 2007, 38, 642-652.	3.0	94
222	Dynamics of Bengal Rose Encapsulated in the Meijer Dendrimer Box. Journal of the American Chemical Society, 1997, 119, 7458-7462.	13.7	93
223	Critical behavior in spallation failure of metals. Physical Review B, 2001, 63, .	3.2	92
224	Optimization and Application of Lithium Parameters for the Reactive Force Field, ReaxFF. Journal of Physical Chemistry A, 2005, 109, 4575-4582.	2.5	92
225	Interactions of Poly(amidoamine) Dendrimers with Human Serum Albumin: Binding Constants and Mechanisms. ACS Nano, 2011, 5, 3456-3468.	14.6	92
226	Design of Covalent Organic Frameworks for Methane Storage. Journal of Physical Chemistry A, 2011, 115, 13852-13857.	2.5	92
227	Ex2Box: Interdependent Modes of Binding in a Two-Nanometer-Long Synthetic Receptor. Journal of the American Chemical Society, 2013, 135, 12736-12746.	13.7	92
228	Electronic Structure of IrO <sub>2</sub> : The Role of the Metal d Orbitals. Journal of Physical Chemistry C, 2015, 119, 11570-11577.	3.1	91
229	Effectively Increased Efficiency for Electroreduction of Carbon Monoxide Using Supported Polycrystalline Copper Powder Electrocatalysts. ACS Catalysis, 2019, 9, 4709-4718.	11.2	91
230	New Foundation for the Use of Pseudopotentials in Metals. Physical Review, 1968, 174, 659-662.	2.7	90
231	Protein simulations using techniques suitable for very large systems: The cell multipole method for nonbond interactions and the Newton-Euler inverse mass operator method for internal coordinate dynamics. Proteins: Structure, Function and Bioinformatics, 1994, 20, 227-247.	2.6	88
232	Predictions of CCR1 Chemokine Receptor Structure and BX 471 Antagonist Binding Followed by Experimental Validation. Journal of Biological Chemistry, 2006, 281, 27613-27620.	3.4	88
233	ReaxFF Reactive Force Field for Solid Oxide Fuel Cell Systems with Application to Oxygen Ion Transport in Yttria-Stabilized Zirconia. Journal of Physical Chemistry A, 2008, 112, 3133-3140.	2.5	88
234	Thermochemistry for Hydrocarbon Intermediates Chemisorbed on Metal Surfaces: CHn-m(CH3)m with n = 1, 2, 3 and m ≤n on Pt, Ir, Os, Pd, Rh, and Ru. Journal of the American Chemical Society, 2000, 122, 2309-2321.	13.7	87

#	Article	IF	CITATIONS
235	Solvent Quality Changes the Structure of G8 PAMAM Dendrimer, a Disagreement with Some Experimental Interpretations. Journal of Physical Chemistry B, 2006, 110, 25628-25632.	2.6	87
236	Discrete Dimers of Redox-Active and Fluorescent Perylene Diimide-Based Rigid Isosceles Triangles in the Solid State. Journal of the American Chemical Society, 2019, 141, 1290-1303.	13.7	87
237	Elucidation of the dynamics for hot-spot initiation at nonuniform interfaces of highly shocked materials. Physical Review B, 2011, 84, .	3.2	85
238	The role of kinetic energy in chemical binding. Theoretica Chimica Acta, 1972, 26, 195-210.	0.8	84
239	Computational Insights on the Challenges for Polymerizing Polar Monomers. Journal of the American Chemical Society, 2002, 124, 10198-10210.	13.7	84
240	DFT Prediction of Oxygen Reduction Reaction on Palladium–Copper Alloy Surfaces. ACS Catalysis, 2014, 4, 1189-1197.	11.2	84
241	Highly Shocked Polymer Bonded Explosives at a Nonplanar Interface: Hot-Spot Formation Leading to Detonation. Journal of Physical Chemistry C, 2013, 117, 26551-26561.	3.1	83
242	Criteria for formation of metallic glasses: The role of atomic size ratio. Journal of Chemical Physics, 2003, 119, 9858-9870.	3.0	81
243	Making Sense of Olfaction through Predictions of the 3-D Structure and Function of Olfactory Receptors. Chemical Senses, 2004, 29, 269-290.	2.0	81
244	Mechanism of Direct Molecular Oxygen Insertion in a Palladium(II)â^'Hydride Bond. Inorganic Chemistry, 2006, 45, 9631-9633.	4.0	81
245	Molecular dynamics for very large systems on massively parallel computers: The MPSim program. Journal of Computational Chemistry, 1997, 18, 501-521.	3.3	80
246	First Principles Calculations of the pKa Values and Tautomers of Isoguanine and Xanthine. Chemical Research in Toxicology, 2003, 16, 1455-1462.	3.3	80
247	Molecular Dynamics Simulations of the Interactions between Platinum Clusters and Carbon Platelets. Journal of Physical Chemistry A, 2008, 112, 1392-1402.	2.5	80
248	Theoretical Description of the STM Images of Alkanes and Substituted Alkanes Adsorbed on Graphite. Journal of Physical Chemistry B, 1997, 101, 5996-6020.	2.6	79
249	Viscosities of liquid metal alloys from nonequilibrium molecular dynamics. Journal of Computer-Aided Materials Design, 2001, 8, 233-243.	0.7	79
250	Hydroxylation Structure and Proton Transfer Reactivity at the Zinc Oxideâ^'Water Interface. Journal of Physical Chemistry C, 2011, 115, 8573-8579.	3.1	79
251	Development of a ReaxFF Reactive Force Field for Ettringite and Study of its Mechanical Failure Modes from Reactive Dynamics Simulations. Journal of Physical Chemistry A, 2012, 116, 3918-3925.	2.5	79
252	Ab Initio Quantum Mechanical Study of the Structures and Energies for the Pseudorotation of 5â€~Dehydroxy Analogues of 2â€~Deoxyribose and Ribose Sugars. Journal of the American Chemical Society, 1999, 121, 985-993.	13.7	78

#	Article	IF	CITATIONS
253	Mechanism of the Aerobic Oxidation of Alcohols by Palladium Complexes of N-Heterocyclic Carbenes. Journal of the American Chemical Society, 2006, 128, 9651-9660.	13.7	77
254	Development of Interatomic ReaxFF Potentials for Au–S–C–H Systems. Journal of Physical Chemistry A, 2011, 115, 10315-10322.	2.5	77
255	Anisotropic shock sensitivity for <i>β</i> -octahydro-1,3,5,7-tetranitro-1,3,5,7-tetrazocine energetic material under compressive-shear loading from ReaxFF-lg reactive dynamics simulations. Journal of Applied Physics, 2012, 111, .	2.5	77
256	Structure, Bonding, and Stability of a Catalytica Platinum(II) Catalyst:Â A Computational Study. Organometallics, 2003, 22, 2057-2068.	2.3	74
257	HierVLS Hierarchical Docking Protocol for Virtual Ligand Screening of Large-Molecule Databases. Journal of Medicinal Chemistry, 2004, 47, 56-71.	6.4	74
258	Single-Site Vanadyl Activation, Functionalization, and Reoxidation Reaction Mechanism for Propane Oxidative Dehydrogenation on the Cubic V4O10Cluster. Journal of Physical Chemistry C, 2007, 111, 5115-5127.	3.1	74
259	Mechanism and Energetics for Complexation of90Y with 1,4,7,10-Tetraazacyclododecane-1,4,7,10-tetraacetic Acid (DOTA), a Model for Cancer Radioimmunotherapy. Journal of the American Chemical Society, 1999, 121, 6142-6151.	13.7	73
260	Synthesis, Structure, and Reactivity of O-Donor Ir(III) Complexes:Â Câ^'H Activation Studies with Benzene. Journal of the American Chemical Society, 2005, 127, 11372-11389.	13.7	73
261	Dendritic Chelating Agents. 2. U(VI) Binding to Poly(amidoamine) and Poly(propyleneimine) Dendrimers in Aqueous Solutions. Environmental Science & Technology, 2008, 42, 1572-1579.	10.0	73
262	Identification of the Selective Sites for Electrochemical Reduction of CO to C <sub>2+</sub> Products on Copper Nanoparticles by Combining Reactive Force Fields, Density Functional Theory, and Machine Learning. ACS Energy Letters, 2018, 3, 2983-2988.	17.4	73
263	Ab initioeffective potentials for silicon. Physical Review B, 1977, 15, 5038-5048.	3.2	72
264	Agostic Interactions and Dissociation in the First Layer of Water on Pt(111). Journal of the American Chemical Society, 2004, 126, 9360-9368.	13.7	72
265	High H <sub>2</sub> Uptake in Li-, Na-, K-Metalated Covalent Organic Frameworks and Metal Organic Frameworks at 298 K. Journal of Physical Chemistry A, 2012, 116, 1621-1631.	2.5	72
266	Structure-Based Sequence Alignment of the Transmembrane Domains of All Human GPCRs: Phylogenetic, Structural and Functional Implications. PLoS Computational Biology, 2016, 12, e1004805.	3.2	72
267	Ab Initio Calculations on the H2+D2=2HD Fourâ€Center Exchange Reaction. I. Elements of the Reaction Surface. Journal of Chemical Physics, 1969, 51, 716-731.	3.0	71
268	Carboxylic Solvents and O-Donor Ligand Effects on CH Activation by Pt(II). Journal of the American Chemical Society, 2006, 128, 7404-7405.	13.7	71
269	High H2 Storage of Hexagonal Metalâ``Organic Frameworks from First-Principles-Based Grand Canonical Monte Carlo Simulations. Journal of Physical Chemistry C, 2008, 112, 13431-13436.	3.1	71
270	Tailoring a Three-Phase Microenvironment for High-Performance Oxygen Reduction Reaction in Proton Exchange Membrane Fuel Cells. Matter, 2020, 3, 1774-1790.	10.0	71

#	Article	lF	CITATIONS
271	Constant Temperature Constrained Molecular Dynamics:  The Newtonâ^'Euler Inverse Mass Operator Method. The Journal of Physical Chemistry, 1996, 100, 10508-10517.	2.9	70
272	Chemisorption of Organics on Platinum. 1. The Interstitial Electron Model. Journal of Physical Chemistry B, 1998, 102, 9481-9491.	2.6	70
273	Mechanism for antibody catalysis of the oxidation of water by singlet dioxygen. Proceedings of the National Academy of Sciences of the United States of America, 2002, 99, 2636-2641.	7.1	70
274	Adsorption of Atomic H and O on the (111) Surface of Pt3Ni Alloys. Journal of Physical Chemistry B, 2004, 108, 8311-8323.	2.6	70
275	Toward Electrochemically Controllable Tristable Three-Station [2]Catenanes. Chemistry - an Asian Journal, 2007, 2, 76-93.	3.3	70
276	DFT Study of Oxygen Reduction Reaction on Os/Pt Core–Shell Catalysts Validated by Electrochemical Experiment. ACS Catalysis, 2015, 5, 1568-1580.	11.2	70
277	Reaction intermediates during operando electrocatalysis identified from full solvent quantum mechanics molecular dynamics. Proceedings of the National Academy of Sciences of the United States of America, 2019, 116, 7718-7722.	7.1	70
278	A detailed model for the decomposition of nitramines: RDX and HMX. Journal of Computer-Aided Materials Design, 2001, 8, 203-212.	0.7	69
279	Chemisorption of (CHxand C2Hy) Hydrocarbons on Pt(111) Clusters and Surfaces from DFT Studies. Journal of Physical Chemistry B, 2005, 109, 297-311.	2.6	69
280	Anisotropic Shock Sensitivity of Cyclotrimethylene Trinitramine (RDX) from Compress-and-Shear Reactive Dynamics. Journal of Physical Chemistry C, 2012, 116, 10198-10206.	3.1	69
281	<scp>G</scp> proteinâ€coupled odorant receptors: From sequence to structure. Protein Science, 2015, 24, 1543-1548.	7.6	69
282	In Silico Design of Highly Selective Mo-V-Te-Nb-O Mixed Metal Oxide Catalysts for Ammoxidation and Oxidative Dehydrogenation of Propane and Ethane. Journal of the American Chemical Society, 2015, 137, 13224-13227.	13.7	68
283	Core Polarization and Hyperfine Structure of the B, C, N, O, and F Atoms. Physical Review, 1969, 182, 48-64.	2.7	67
284	Fluorinated Imidazoles as Proton Carriers for Water-Free Fuel Cell Membranes. Journal of the American Chemical Society, 2004, 126, 15644-15645.	13.7	67
285	Conformation and Proton Configuration of Pyrimidine Deoxynucleoside Oxidation Damage Products in Water. Chemical Research in Toxicology, 2000, 13, 462-470.	3.3	66
286	Mechanical properties of connected carbon nanorings via molecular dynamics simulation. Physical Review B, 2005, 72, .	3.2	65
287	Modeling the human PTC bitter-taste receptor interactions with bitter tastants. Journal of Molecular Modeling, 2006, 12, 931-941.	1.8	65
288	Compressive Shear Reactive Molecular Dynamics Studies Indicating That Cocrystals of TNT/CL-20 Decrease Sensitivity, Journal of Physical Chemistry C, 2014, 118, 30202-30208	3.1	65

#	Article	IF	CITATIONS
289	Folding of Oligoviologens Induced by Radical–Radical Interactions. Journal of the American Chemical Society, 2015, 137, 876-885.	13.7	65
290	Wavefunctions and Correlation Energies for Twoâ€, Threeâ€, and Fourâ€Electron Atoms. Journal of Chemical Physics, 1968, 48, 1008-1017.	3.0	64
291	How broadly tuned olfactory receptors equally recognize their agonists. Human OR1G1 as a test case. Cellular and Molecular Life Sciences, 2012, 69, 4205-4213.	5.4	64
292	First-Principles-Based Reaction Kinetics for Decomposition of Hot, Dense Liquid TNT from ReaxFF Multiscale Reactive Dynamics Simulations. Journal of Physical Chemistry C, 2013, 117, 21043-21054.	3.1	64
293	Au-activated N motifs in non-coherent cupric porphyrin metal organic frameworks for promoting and stabilizing ethylene production. Nature Communications, 2022, 13, 63.	12.8	64
294	Theoretical evidence for bound electronic excited states of ozone. Chemical Physics Letters, 1973, 23, 457-462.	2.6	63
295	Dramatic differences in carbon dioxide adsorption and initial steps of reduction between silver and copper. Nature Communications, 2019, 10, 1875.	12.8	63
296	Nanophase Segregation and Water Dynamics in the Dendrion Diblock Copolymer Formed from the Fréchet Polyaryl Ethereal Dendrimer and Linear PTFE. Journal of Physical Chemistry B, 2005, 109, 10154-10167.	2.6	62
297	Inaccessibility of β-Hydride Elimination from â^'OH Functional Groups in Wacker-Type Oxidation. Journal of the American Chemical Society, 2006, 128, 3132-3133.	13.7	62
298	Atomic-Level Simulations of Seeman DNA Nanostructures: The Paranemic Crossover in Salt Solution. Biophysical Journal, 2006, 90, 1463-1479.	0.5	61
299	Dearomatization Reactions of N-Heterocycles Mediated by Group 3 Complexes. Journal of the American Chemical Society, 2010, 132, 342-355.	13.7	61
300	Unraveling Structural Models of Graphite Fluorides by Density Functional Theory Calculations. Chemistry of Materials, 2010, 22, 2142-2154.	6.7	60
301	New Type of Wave Function for Li,Be+, andB++. Physical Review, 1968, 169, 120-130.	2.7	59
302	The ReaxFF Monte Carlo Reactive Dynamics Method for Predicting Atomistic Structures of Disordered Ceramics: Application to the Mo <sub>3</sub> VO <sub><i>x</i></sub> Catalyst. Angewandte Chemie - International Edition, 2009, 48, 7630-7634.	13.8	59
303	Cyclooctyne-based reagents for uncatalyzed click chemistry: A computational survey. Organic and Biomolecular Chemistry, 2009, 7, 5255.	2.8	58
304	Predicted 3D structures for adenosine receptors bound to ligands: Comparison to the crystal structure. Journal of Structural Biology, 2010, 170, 10-20.	2.8	58
305	Predicted Optimal Bifunctional Electrocatalysts for the Hydrogen Evolution Reaction and the Oxygen Evolution Reaction Using Chalcogenide Heterostructures Based on Machine Learning Analysis of in Silico Quantum Mechanics Based High Throughput Screening. Journal of Physical Chemistry Letters, 2020, 11, 869-876.	4.6	58
306	Molecular modelling of dendrimers for nanoscale applications. Nanotechnology, 2000, 11, 77-84.	2.6	57

#	Article	IF	CITATIONS
307	Zeolitic Imidazolate Frameworks as H2 Adsorbents: Ab Initio Based Grand Canonical Monte Carlo Simulation. Journal of Physical Chemistry C, 2010, 114, 12039-12047.	3.1	57
308	Experimental Sabatier plot for predictive design of active and stable Pt-alloy oxygen reduction reaction catalysts. Nature Catalysis, 2022, 5, 513-523.	34.4	57
309	Nonlinear partial differential equations and applications: Peroxone chemistry: Formation of H2O3 and ring-(HO2)(HO3) from O3/H2O2. Proceedings of the National Academy of Sciences of the United States of America, 2002, 99, 15308-15312.	7.1	56
310	Structures, Mechanisms, and Kinetics of Selective Ammoxidation and Oxidation of Propane over Multi-metal Oxide Catalysts. Topics in Catalysis, 2008, 50, 2-18.	2.8	56
311	Experimentally-Based Recommendations of Density Functionals for Predicting Properties in Mechanically Interlocked Molecules. Journal of the American Chemical Society, 2008, 130, 14928-14929.	13.7	56
312	Friction anisotropy at Ni(100)/(100) interfaces: Molecular dynamics studies. Physical Review B, 2002, 66,	3.2	55
313	Development of a ReaxFF Reactive Force Field for Aqueous Chloride and Copper Chloride. Journal of Physical Chemistry A, 2010, 114, 3556-3568.	2.5	55
314	Anions dramatically enhance proton transfer through aqueous interfaces. Proceedings of the National Academy of Sciences of the United States of America, 2012, 109, 10228-10232.	7.1	55
315	Redox Control of the Binding Modes of an Organic Receptor. Journal of the American Chemical Society, 2015, 137, 11057-11068.	13.7	55
316	Atomistic Explanation of the Dramatically Improved Oxygen Reduction Reaction of Jagged Platinum Nanowires, 50 Times Better than Pt. Journal of the American Chemical Society, 2020, 142, 8625-8632.	13.7	55
317	The theoretical study on interaction of hydrogen with single-walled boron nitride nanotubes. I. The reactive force field ReaxFFHBN development. Journal of Chemical Physics, 2005, 123, 114703.	3.0	54
318	Reactions of Group III Biheterocyclic Complexes. Journal of the American Chemical Society, 2009, 131, 10269-10278.	13.7	54
319	Structures, Energetics, and Reaction Barriers for CHx Bound to the Nickel (111) Surface. Journal of Physical Chemistry C, 2009, 113, 20290-20306.	3.1	54
320	Mechanism of O <sub>2</sub> Activation and Methanol Production by (Di(2-pyridyl)methanesulfonate)Pt <sup>II</sup> Me(OH <sub><i>n</i></sub> ) <sup>(2–<i>n</i>)–</sup> Complex from Theory with Validation from Experiment. Journal of the American Chemical Society, 2014, 136, 2335-2341.	13.7	54
321	The orbital description of the potential energy curves and properties of the lower excited states of the BH molecule. Chemical Physics, 1974, 3, 297-316.	1.9	53
322	Prediction of the 3D Structure and Dynamics of Human DP G-Protein Coupled Receptor Bound to an Agonist and an Antagonist. Journal of the American Chemical Society, 2007, 129, 10720-10731.	13.7	53
323	Donor–Acceptor Oligorotaxanes Made to Order. Chemistry - A European Journal, 2011, 17, 2107-2119.	3.3	53
324	Adaptive Accelerated ReaxFF Reactive Dynamics with Validation from Simulating Hydrogen Combustion. Journal of the American Chemical Society, 2014, 136, 9434-9442.	13.7	53

#	Article	IF	CITATIONS
325	The atomistic origin of the extraordinary oxygen reduction activity of Pt <sub>3</sub> Ni <sub>7</sub> fuel cell catalysts. Chemical Science, 2015, 6, 3915-3925.	7.4	53
326	Electronic Structure of LiH According to a Generalization of the Valenceâ€Bond Method. Journal of Chemical Physics, 1969, 50, 4524-4532.	3.0	52
327	Benzene Câ^'H Bond Activation in Carboxylic Acids Catalyzed by O-Donor Iridium(III) Complexes: An Experimental and Density Functional Study. Organometallics, 2010, 29, 742-756.	2.3	52
328	Probing the C–O Bond-Formation Step in Metalloporphyrin-Catalyzed C–H Oxygenation Reactions. ACS Catalysis, 2017, 7, 4182-4188.	11.2	52
329	The incorporation of quadratic convergence into open-shell self-consistent field equations. Chemical Physics Letters, 1970, 6, 147-151.	2.6	51
330	Electron-phonon interactions and superconductivity inK3C60. Physical Review B, 1993, 48, 13959-13970.	3.2	51
331	Structures and Transport Properties of Hydrated Water-Soluble Dendrimer-Grafted Polymer Membranes for Application to Polymer Electrolyte Membrane Fuel Cells:  Classical Molecular Dynamics Approach. Journal of Physical Chemistry C, 2007, 111, 2759-2769.	3.1	51
332	Predicted structure of agonist-bound glucagon-like peptide 1 receptor, a class B G protein-coupled receptor. Proceedings of the National Academy of Sciences of the United States of America, 2012, 109, 19988-19993.	7.1	51
333	Design of a Graphene Nitrene Two-Dimensional Catalyst Heterostructure Providing a Well-Defined Site Accommodating One to Three Metals, with Application to CO <sub>2</sub> Reduction Electrocatalysis for the Two-Metal Case. Journal of Physical Chemistry Letters, 2020, 11, 2541-2549.	4.6	51
334	Pd-Mediated Activation of Molecular Oxygen:Â Pd(0) versus Direct Insertion. Journal of the American Chemical Society, 2007, 129, 10361-10369.	13.7	50
335	Compressed Intermetallic PdCu for Enhanced Electrocatalysis. ACS Energy Letters, 2020, 5, 3672-3680.	17.4	50
336	Magnetic Hyperfine Structure of Lithium. Physical Review, 1967, 157, 93-96.	2.7	49
337	Heterolytic CH Activation with a Cyclometalated Platinum(II) 6-Phenyl-4,4â€ <sup>~</sup> -di-tert-butyl-2,2-Bipyridine Complex. Organometallics, 2006, 25, 4734-4737.	2.3	48
338	Computational modeling of structure and OH-anion diffusion in quaternary ammonium polysulfone hydroxide – Polymer electrolyte for application in electrochemical devices. Journal of Membrane Science, 2013, 431, 79-85.	8.2	48
339	Alkylation of Phenol:Â A Mechanistic View. Journal of Physical Chemistry A, 2006, 110, 2246-2252.	2.5	47
340	Methylrhenium Trioxide Revisited:  Mechanisms for Nonredox Oxygen Insertion in an Mâ^'CH3 Bond. Journal of the American Chemical Society, 2007, 129, 15794-15804.	13.7	47
341	Predictions of melting, crystallization, and local atomic arrangements of aluminum clusters using a reactive force field. Journal of Chemical Physics, 2008, 129, 244506.	3.0	47
342	De Novo Ultrascale Atomistic Simulations On High-End Parallel Supercomputers. International Journal of High Performance Computing Applications, 2008, 22, 113-128.	3.7	47

#	Article	IF	CITATIONS
343	DNA-Linker-Induced Surface Assembly of Ultra Dense Parallel Single Walled Carbon Nanotube Arrays. Nano Letters, 2012, 12, 1129-1135.	9.1	47
344	Universal Correction of Density Functional Theory to Include London Dispersion (up to Lr, Element) Tj ETQq0 0 0	rgBT /Ove 4.6	erlock 10 Tf 5
345	Oligorotaxane Radicals under Orders. ACS Central Science, 2016, 2, 89-98.	11.3	47
346	The low-lying excited states of water, methanol, and dimethyl ether. Chemical Physics, 1976, 18, 1-11.	1.9	46
347	Dynamic friction force in a carbon peapod oscillator. Nanotechnology, 2006, 17, 5691-5695.	2.6	46
348	Structure of polyamidoamide dendrimers up to limiting generations: A mesoscale description. Journal of Chemical Physics, 2009, 130, 144902.	3.0	46
349	Hydrophobic Segregation, Phase Transitions and the Anomalous Thermodynamics of Water/Methanol Mixtures. Journal of Physical Chemistry B, 2012, 116, 13905-13912.	2.6	46
350	Role of solvent-anion charge transfer in oxidative degradation of battery electrolytes. Nature Communications, 2019, 10, 3360.	12.8	46
351	Improved Quantum Theory of Manyâ€Electron Systems. IV. Properties of GF Wavefunctions. Journal of Chemical Physics, 1968, 48, 5337-5347.	3.0	45
352	Charge density waves, spin density waves, and Peierls distortions in oneâ€dimensional metals. I. Hartree–Fock studies of Cu, Ag, Au, Li, and Na. Journal of Chemical Physics, 1988, 88, 277-302.	3.0	45
353	Band structures of II-VI semiconductors using Gaussian basis functions with separableab initiopseudopotentials: Application to prediction of band offsets. Physical Review B, 1996, 53, 1377-1387.	3.2	45
354	A theoretical study of the conversion of gas phase methanediol to formaldehyde. Journal of Chemical Physics, 2003, 119, 5117-5120.	3.0	45
355	Dendritic Anion Hosts:  Perchlorate Uptake by G5-NH <sub>2</sub> Poly(propyleneimine) Dendrimer in Water and Model Electrolyte Solutions. Environmental Science & Technology, 2007, 41, 6521-6527.	10.0	45
356	Flat-Bottom Strategy for Improved Accuracy in Protein Side-Chain Placements. Journal of Chemical Theory and Computation, 2008, 4, 2160-2169.	5.3	45
357	Singlet–triplet energy gaps in fluorineâ€substituted methylenes and silylenes. Journal of Chemical Physics, 1990, 93, 4986-4993.	3.0	44
358	Effects of Molecular Geometry on the STM Image Contrast of Methyl- and Bromo-Substituted Alkanes and Alkanols on Graphite. Journal of Physical Chemistry B, 1999, 103, 9690-9699.	2.6	44

359	Theoretical study on interaction of hydrogen with single-walled boron nitride nanotubes. II. Collision, storage, and adsorption. Journal of Chemical Physics, 2005, 123, 114704.	3.0	44
360	Functionally Rigid and Degenerate Molecular Shuttles. Chemistry - A European Journal, 2009, 15, 1115-1122.	3.3	44

#	Article	IF	CITATIONS
361	Absolute Entropy and Energy of Carbon Dioxide Using the Two-Phase Thermodynamic Model. Journal of Chemical Theory and Computation, 2011, 7, 1893-1901.	5.3	44
362	Bihelix: Towards <i>de novo</i> structure prediction of an ensemble of Gâ€protein coupled receptor conformations. Proteins: Structure, Function and Bioinformatics, 2012, 80, 505-518.	2.6	44
363	Ab initio theoretical results on the stability of cyclic ozone. Journal of Chemical Physics, 1977, 67, 2377.	3.0	43
364	The low lying states of ammonia; generalized valence bond and configuration interaction studies. Chemical Physics, 1977, 19, 131-136.	1.9	43
365	Test of the Binding Threshold Hypothesis for olfactory receptors: Explanation of the differential binding of ketones to the mouse and human orthologs of olfactory receptor 912-93. Protein Science, 2005, 14, 703-710.	7.6	43
366	Dynamic behavior of fully solvated beta2-adrenergic receptor, embedded in the membrane with bound agonist or antagonist. Proceedings of the National Academy of Sciences of the United States of America, 2006, 103, 4882-4887.	7.1	43
367	Functional selectivity of dopamine D1 receptor agonists in regulating the fate of internalized receptors. Neuropharmacology, 2007, 52, 562-575.	4.1	43
368	Nucleation of amorphous shear bands at nanotwins in boron suboxide. Nature Communications, 2016, 7, 11001.	12.8	43
369	Polarizable charge equilibration model for predicting accurate electrostatic interactions in molecules and solids. Journal of Chemical Physics, 2017, 146, 124117.	3.0	43
370	Electrochemical Switching of a Fluorescent Molecular Rotor Embedded within a Bistable Rotaxane. Journal of the American Chemical Society, 2020, 142, 11835-11846.	13.7	43
371	The DFT-ReaxFF Hybrid Reactive Dynamics Method with Application to the Reductive Decomposition Reaction of the TFSI and DOL Electrolyte at a Lithium–Metal Anode Surface. Journal of Physical Chemistry Letters, 2021, 12, 1300-1306.	4.6	43
372	Exchange kinetic energy, contragradience, and chemical binding. Chemical Physics Letters, 1970, 5, 45-49.	2.6	42
373	Atomic simulations of kinetic friction and its velocity dependence atAlâ^•Alandαâ^'Al2O3â^•αâ^'Al2O3interfaces. Physical Review B, 2005, 72, .	3.2	42
374	Annealing kinetics of electrodeposited lithium dendrites. Journal of Chemical Physics, 2015, 143, 134701.	3.0	42
375	Correlation Analysis of Chemical Bonds. Journal of Physical Chemistry A, 1998, 102, 2919-2933.	2.5	41
376	Multiscale modeling and simulation methods with applications to dendritic polymers. Computational and Theoretical Polymer Science, 2001, 11, 345-356.	1.1	41
377	Characterization of the active site of yeast RNA polymerase II by DFT and ReaxFF calculations. Theoretical Chemistry Accounts, 2008, 120, 479-489.	1.4	41
378	Modeling High Rate Impact Sensitivity of Perfect RDX and HMX Crystals by ReaxFF Reactive Dynamics. Journal of Energetic Materials, 2010, 28, 92-127.	2.0	41

#	Article	IF	CITATIONS
379	Reactivity of a Series of Isostructural Cobalt Pincer Complexes with CO <sub>2</sub> , CO, and H <sup>+</sup> . Inorganic Chemistry, 2014, 53, 13031-13041.	4.0	41
380	CO <sub>2</sub> reduction on pure Cu produces only H <sub>2</sub> after subsurface O is depleted: Theory and experiment. Proceedings of the National Academy of Sciences of the United States of America, 2021, 118, .	7.1	41
381	Electronic states of silicon vacancy. I. Covalent states. Physical Review B, 1978, 18, 2831-2839.	3.2	40
382	Stabilization of α-Helices by Dipoleâ^'Dipole Interactions within α-Helices. Journal of Physical Chemistry B, 2000, 104, 7784-7789.	2.6	40
383	Superprotonic phase transition ofCsHSO4: A molecular dynamics simulation study. Physical Review B, 2005, 72, .	3.2	40
384	ReaxFF Reactive Force-Field Modeling of the Triple-Phase Boundary in a Solid Oxide Fuel Cell. Journal of Physical Chemistry Letters, 2014, 5, 4039-4043.	4.6	40
385	Accurate Ab Initio Quantum Mechanics Simulations of Bi <sub>2</sub> Se <sub>3</sub> and Bi <sub>2</sub> Te <sub>3</sub> Topological Insulator Surfaces. Journal of Physical Chemistry Letters, 2015, 6, 3792-3796.	4.6	40
386	Role of Ligand Protonation in Dihydrogen Evolution from a Pentamethylcyclopentadienyl Rhodium Catalyst. Inorganic Chemistry, 2017, 56, 11375-11386.	4.0	40
387	Atomistic Simulations of Corrosion Inhibitors Adsorbed on Calcite Surfaces I. Force field Parameters for Calcite. Journal of Physical Chemistry B, 2001, 105, 10746-10752.	2.6	39
388	First-Principles-Based Dispersion Augmented Density Functional Theory: From Molecules to Crystals. Journal of Physical Chemistry Letters, 2010, 1, 2550-2555.	4.6	39
389	Toward a Process-Based Molecular Model of SiC Membranes. 1. Development of a Reactive Force Field. Journal of Physical Chemistry C, 2013, 117, 3308-3319.	3.1	39
390	Size-Matched Radical Multivalency. Journal of the American Chemical Society, 2017, 139, 3986-3998.	13.7	39
391	Free Energy Barrier for Molecular Motions in Bistable [2]Rotaxane Molecular Electronic Devices. Journal of Physical Chemistry A, 2009, 113, 2136-2143.	2.5	38
392	Mechanism for Activation of Molecular Oxygen by <i>cis</i> - and <i>trans</i> -(Pyridine) <sub>2</sub> Pd(OAc)H: Pd <sup>0</sup> versus Direct Insertion. Journal of the American Chemical Society, 2009, 131, 1416-1425.	13.7	38
393	Equilibrium 2H/1H fractionations in organic molecules: I. Experimental calibration of ab initio calculations. Geochimica Et Cosmochimica Acta, 2009, 73, 7060-7075.	3.9	38
394	Mechanisms Underlying the Mpemba Effect in Water from Molecular Dynamics Simulations. Journal of Physical Chemistry C, 2015, 119, 2622-2629.	3.1	38
395	Influence of Elastic Deformation on Single-Wall Carbon Nanotube Atomic Force Microscopy Probe Resolution. Journal of Physical Chemistry B, 2004, 108, 13613-13618.	2.6	37
396	3-Dimensional Structures of G Protein-Coupled Receptors and Binding Sites of Agonists and Antagonists. Journal of Nutrition, 2007, 137, 1528S-1538S.	2.9	37

#	Article	IF	CITATIONS
397	Time Resolved Studies of Interfacial Reactions of Ozone with Pulmonary Phospholipid Surfactants Using Field Induced Droplet Ionization Mass Spectrometry. Journal of Physical Chemistry B, 2010, 114, 9496-9503.	2.6	37
398	Improved H <sub>2</sub> Storage in Zeolitic Imidazolate Frameworks Using Li <sup>+</sup> , Na <sup>+</sup> , and K <sup>+</sup> Dopants, with an Emphasis on Delivery H <sub>2</sub> Uptake. Journal of Physical Chemistry C, 2011, 115, 3507-3512.	3.1	37
399	Structure-Based Prediction of Subtype Selectivity of Histamine H <sub>3</sub> Receptor Selective Antagonists in Clinical Trials. Journal of Chemical Information and Modeling, 2011, 51, 3262-3274.	5.4	37
400	Highly Selective Electrocatalytic Reduction of CO <sub>2</sub> into Methane on Cu–Bi Nanoalloys. Journal of Physical Chemistry Letters, 2020, 11, 7261-7266.	4.6	37
401	Reaction Mechanism, Origins of Enantioselectivity, and Reactivity Trends in Asymmetric Allylic Alkylation: A Comprehensive Quantum Mechanics Investigation of a C(sp <sup>3</sup> )–C(sp <sup>3</sup> ) Cross-Coupling. Journal of the American Chemical Society, 2020, 142, 13917-13933.	13.7	37
402	The Rydberg states of trans-butadiene from generalized valence bond and configuration interaction calculations. Chemical Physics, 1980, 53, 251-263.	1.9	36
403	Dual-space approach for density-functional calculations of two- and three-dimensional crystals using Gaussian basis functions. Physical Review B, 1995, 52, 2348-2361.	3.2	36
404	Chelators for Radioimmunotherapy:Â I. NMR and Ab Initio Calculation Studies on 1,4,7,10-Tetra(carboxyethyl)-1,4,7,10-tetraazacyclododecane (DO4Pr) and 1,4,7-Tris(carboxymethyl)-10-(carboxyethyl)-1,4,7,10-tetraazacyclododecane (DO3A1Pr). Inorganic Chemistry, 2001, 40, 4310-4318.	4.0	36
405	Strategies for multiscale modeling and simulation of organic materials: polymers and biopolymers. Computational and Theoretical Polymer Science, 2001, 11, 329-343.	1.1	36
406	The Role of Confined Water in Ionic Liquid Electrolytes for Dye-Sensitized Solar Cells. Journal of Physical Chemistry Letters, 2012, 3, 556-559.	4.6	36
407	Studies of fullerenes and carbon nanotubes by an extended bond order potential. Nanotechnology, 1999, 10, 263-268.	2.6	35
408	Secondary Organic Aerosol Formation by Heterogeneous Reactions of Aldehydes and Ketones:Â A Quantum Mechanical Study. Environmental Science & Technology, 2006, 40, 2333-2338.	10.0	35
409	Parametrization of a reactive force field for aluminum hydride. Journal of Chemical Physics, 2009, 131, 044501.	3.0	35
410	Generalized valence bond wave functions in quantum Monte Carlo. Journal of Chemical Physics, 2010, 132, 164110.	3.0	35
411	Chemistry in the Center for Catalytic Hydrocarbon Functionalization: An Energy Frontier Research Center. Catalysis Letters, 2011, 141, 213-221.	2.6	35
412	Prediction of the Chapman–Jouguet chemical equilibrium state in a detonation wave from first principles based reactive molecular dynamics. Physical Chemistry Chemical Physics, 2016, 18, 2015-2022.	2.8	35
413	Multilayer Two-Dimensional Water Structure Confined in MoS <sub>2</sub> . Journal of Physical Chemistry C, 2017, 121, 16021-16028.	3.1	35
414	Magnetic Hyperfine Structure and Core Polarization in the Excited States of Lithium. Physical Review, 1968, 176, 106-114.	2.7	34

#	Article	IF	CITATIONS
415	Theoretical studies of the dissociative adsorption of H2 on Ni(001) using ab initio parameterized LEPS calculations. Surface Science, 1980, 95, 391-402.	1.9	34
416	Mechanism of Oxidative Shuttling for [2]Rotaxane in a Stoddartâ^'Heath Molecular Switch:  Density Functional Theory Study with Continuum-Solvation Model. Journal of Physical Chemistry B, 2006, 110, 7660-7665.	2.6	34
417	Competing, Coverage-Dependent Decomposition Pathways for C <sub>2</sub> H <sub><i>y</i></sub> Species on Nickel (111). Journal of Physical Chemistry C, 2010, 114, 20028-20041.	3.1	34
418	Interaction of e. coli outer-membrane protein A with sugars on the receptors of the brain microvascular endothelial cells. Proteins: Structure, Function and Bioinformatics, 2002, 50, 213-221.	2.6	33
419	The Predicted 3D Structures of the Human M1 Muscarinic Acetylcholine Receptor with Agonist or Antagonist Bound. ChemMedChem, 2006, 1, 878-890.	3.2	33
420	Predicted Optimum Composition for the Glass-Forming Ability of Bulk Amorphous Alloys: Application to Cu–Zr–Al. Journal of Physical Chemistry Letters, 2012, 3, 3143-3148.	4.6	33
421	Dramatic Increase in the Oxygen Reduction Reaction for Platinum Cathodes from Tuning the Solvent Dielectric Constant. Angewandte Chemie - International Edition, 2014, 53, 6669-6672.	13.8	33
422	Sliding-Ring Catenanes. Journal of the American Chemical Society, 2016, 138, 10214-10225.	13.7	33
423	CO Coupling Chemistry of a Terminal Mo Carbide: Sequential Addition of Proton, Hydride, and CO Releases Ethenone. Journal of the American Chemical Society, 2019, 141, 15664-15674.	13.7	33
424	Autobifunctional Mechanism of Jagged Pt Nanowires for Hydrogen Evolution Kinetics via End-to-End Simulation. Journal of the American Chemical Society, 2021, 143, 5355-5363.	13.7	33
425	Virtual Screening for Binding of Phenylalanine Analogues to Phenylalanyl-tRNA Synthetase. Journal of the American Chemical Society, 2002, 124, 14442-14449.	13.7	32
426	The structure of human serotonin 2c C-protein-coupled receptor bound to agonists and antagonists. Journal of Molecular Graphics and Modelling, 2008, 27, 66-81.	2.4	32
427	Interfacial Thermodynamics of Water and Six Other Liquid Solvents. Journal of Physical Chemistry B, 2014, 118, 5943-5956.	2.6	32
428	QM-Mechanism-Based Hierarchical High-Throughput in Silico Screening Catalyst Design for Ammonia Synthesis. Journal of the American Chemical Society, 2018, 140, 17702-17710.	13.7	32
429	Effects of High and Low Salt Concentrations in Electrolytes at Lithium–Metal Anode Surfaces Using DFT-ReaxFF Hybrid Molecular Dynamics Method. Journal of Physical Chemistry Letters, 2021, 12, 2922-2929.	4.6	32
430	A multiscale approach for modeling crystalline solids. Journal of Computer-Aided Materials Design, 2001, 8, 127-149.	0.7	31
431	Molecular dynamics simulations to compute the bulk response of amorphous PMMA. Journal of Computer-Aided Materials Design, 2001, 8, 87-106.	0.7	31
432	Nanopores of carbon nanotubes as practical hydrogen storage media. Applied Physics Letters, 2005, 87, 213113.	3.3	31

#	Article	IF	CITATIONS
433	Experimental and quantum mechanics investigations of early reactions of monomethylhydrazine with mixtures of NO2 and N2O4. Combustion and Flame, 2013, 160, 970-981.	5.2	31
434	Interface Structure in Li-Metal/[Pyr <sub>14</sub> ][TFSI]-Ionic Liquid System from ab Initio Molecular Dynamics Simulations. Journal of Physical Chemistry Letters, 2019, 10, 4577-4586.	4.6	31
435	Liquefaction of H2 molecules upon exterior surfaces of carbon nanotube bundles. Applied Physics Letters, 2005, 86, 203108.	3.3	30
436	Mechanistic Investigation of Iridium-Catalyzed Hydrovinylation of Olefins. Organometallics, 2006, 25, 1618-1625.	2.3	30
437	Origin of static friction and its relationship to adhesion at the atomic scale. Physical Review B, 2007, 75, .	3.2	30
438	Experimental Validation of the Predicted Binding Site of Escherichia coli K1 Outer Membrane Protein A to Human Brain Microvascular Endothelial Cells. Journal of Biological Chemistry, 2010, 285, 37753-37761.	3.4	30
439	Predicted structures of agonist and antagonist bound complexes of adenosine A <sub>3</sub> receptor. Proteins: Structure, Function and Bioinformatics, 2011, 79, 1878-1897.	2.6	30
440	Measurement of the ground-state distributions in bistable mechanically interlocked molecules using slow scan rate cyclic voltammetry. Proceedings of the National Academy of Sciences of the United States of America, 2011, 108, 20416-20421.	7.1	30
441	Deswelling Mechanisms of Surface-Grafted Poly(NIPAAm) Brush: Molecular Dynamics Simulation Approach. Journal of Physical Chemistry C, 2012, 116, 15974-15985.	3.1	30
442	Nanocomposites of Tantalumâ€Based Pyrochlore and Indium Hydroxide Showing High and Stable Photocatalytic Activities for Overall Water Splitting and Carbon Dioxide Reduction. Angewandte Chemie - International Edition, 2014, 53, 14216-14220.	13.8	30
443	Mechanisms and energetics of free radical initiated disulfide bond cleavage in model peptides and insulin by mass spectrometry. Chemical Science, 2015, 6, 4550-4560.	7.4	30
444	Nanotwins soften boron-rich boron carbide (B13C2). Applied Physics Letters, 2017, 110, .	3.3	30
445	Transport of hot carriers in plasmonic nanostructures. Physical Review Materials, 2019, 3, .	2.4	30
446	The excited electronic states of all-trans-1,3,5-hexatriene. Chemical Physics Letters, 1979, 60, 197-200.	2.6	29
447	Aminomethanol water elimination: Theoretical examination. Journal of Chemical Physics, 2005, 123, 034304.	3.0	29
448	Modeling the sorption dynamics of NaH using a reactive force field. Journal of Chemical Physics, 2008, 128, 164714.	3.0	29
449	Influence of Constitution and Charge on Radical Pairing Interactions in Tris-radical Tricationic Complexes. Journal of the American Chemical Society, 2016, 138, 8288-8300.	13.7	29
450	The Oxygen Reduction Reaction on Graphene from Quantum Mechanics: Comparing Armchair and Zigzag Carbon Edges. Journal of Physical Chemistry C, 2017, 121, 24408-24417.	3.1	29

#	Article	IF	CITATIONS
451	First-principles–based reaction kinetics from reactive molecular dynamics simulations: Application to hydrogen peroxide decomposition. Proceedings of the National Academy of Sciences of the United States of America, 2019, 116, 18202-18208.	7.1	29
452	Artificial Intelligence and QM/MM with a Polarizable Reactive Force Field for Next-Generation Electrocatalysts. Matter, 2021, 4, 195-216.	10.0	29
453	New Approach to Energy-Band Calculations with Results for Lithium Metal. Physical Review Letters, 1969, 23, 300-303.	7.8	28
454	A generalized direct inversion in the iterative subspace approach for generalized valence bond wave functions. Journal of Chemical Physics, 1994, 100, 1226-1235.	3.0	28
455	Design of a nanomechanical fluid control valve based on functionalized silicon cantilevers: coupling molecular mechanics with classical engineering design. Nanotechnology, 2004, 15, 1405-1415.	2.6	28
456	The MPSim-Dock hierarchical docking algorithm: Application to the eight trypsin inhibitor cocrystals. Journal of Computational Chemistry, 2005, 26, 48-71.	3.3	28
457	ReaxFF Monte Carlo reactive dynamics: Application to resolving the partial occupations of the M1 phase of the MoVNbTeO catalyst. Catalysis Today, 2010, 157, 71-76.	4.4	28
458	Predicted Structures and Dynamics for Agonists and Antagonists Bound to Serotonin 5-HT2B and 5-HT2C Receptors. Journal of Chemical Information and Modeling, 2011, 51, 420-433.	5.4	28
459	Initial Decomposition of HMX Energetic Material from Quantum Molecular Dynamics and the Molecular Structure Transition of β-HMX to δ-HMX. Journal of Physical Chemistry C, 2019, 123, 9231-9236.	3.1	28
460	Si-Doped Fe Catalyst for Ammonia Synthesis at Dramatically Decreased Pressures and Temperatures. Journal of the American Chemical Society, 2020, 142, 8223-8232.	13.7	28
461	Dipole moments and electric field gradients for correlated wavefunctions of NO: The X 2 Î, A 2 Σ + , and D 2 Σ + states. Chemical Physics Letters, 1975, 33, 18-24.	2.6	27
462	New concepts of bonding in nonperiodic metallic systems. Journal of Non-Crystalline Solids, 1985, 75, 149-159.	3.1	27
463	Predicting glycosaminoglycan surface protein interactions and implications for studying axonal growth. Proceedings of the National Academy of Sciences of the United States of America, 2017, 114, 13697-13702.	7.1	27
464	The quantum mechanics-based polarizable force field for water simulations. Journal of Chemical Physics, 2018, 149, 174502.	3.0	27
465	Reaction mechanism and kinetics for ammonia synthesis on the Fe(211) reconstructed surface. Physical Chemistry Chemical Physics, 2019, 21, 11444-11454.	2.8	27
466	Optimal spline cutoffs for Coulomb and van der Waals interactions. Chemical Physics Letters, 1992, 193, 197-201.	2.6	26
467	Assessment of phenomenological models for viscosity of liquids based on nonequilibrium atomistic simulations of copper. Journal of Chemical Physics, 2005, 123, 104506.	3.0	26
468	Bifunctional Anchors Connecting Carbon Nanotubes to Metal Electrodes for Improved Nanoelectronics. Journal of the American Chemical Society, 2007, 129, 9834-9835.	13.7	26

#	Article	IF	CITATIONS
469	Concerning the Stability of the Negative IonsHâ^'andLiâ^'. Physical Review, 1968, 172, 7-12.	2.7	25
470	Conduction properties of the organic superconductorκâ^'(BEDTâ^'TTF)2Cu(NCS)2based on Hubbard–unrestricted-Hartree-Fock band calculations. Physical Review B, 1997, 56, 11907-11919.	3.2	25
471	Application of the Self-Assembled Monolayer (SAM) Model to Dithiophosphate and Dithiocarbamate Engine Wear Inhibitors. Journal of Physical Chemistry A, 2000, 104, 2508-2524.	2.5	25
472	Partitioning of Poly(amidoamine) Dendrimers between n-Octanol and Water. Environmental Science & Technology, 2009, 43, 5123-5129.	10.0	25
473	The lower electronic states of MoN. Chemical Physics, 1983, 81, 263-271.	1.9	24
474	Tunneling Mechanism Implications from an STM Study of H3C(CH2)15HCCCH(CH2)15CH3 on Graphite and C14H29OH on MoS2. Journal of Physical Chemistry B, 1999, 103, 7077-7080.	2.6	24
475	Prediction of the 3D Structure of FMRFâ€amide Neuropeptides Bound to the Mouse MrgC11 GPCR and Experimental Validation. ChemBioChem, 2007, 8, 1527-1539.	2.6	24
476	Molecular Dynamics Simulations of Metal Clusters Supported on Fishbone Carbon Nanofibers. Journal of Physical Chemistry C, 2010, 114, 3522-3530.	3.1	24
477	DFT Virtual Screening Identifies Rhodium–Amidinate Complexes As Potential Homogeneous Catalysts for Methane-to-Methanol Oxidation. ACS Catalysis, 2014, 4, 4455-4465.	11.2	24
478	Rhodium Bis(quinolinyl)benzene Complexes for Methane Activation and Functionalization. Chemistry - A European Journal, 2015, 21, 1286-1293.	3.3	24
479	Pressureâ€Dependent Polymorphism and Bandâ€Gap Tuning of Methylammonium Lead Iodide Perovskite. Angewandte Chemie, 2016, 128, 6650-6654.	2.0	24
480	Prediction of the crystal packing of diâ€ŧetrazineâ€ŧetroxide (DTTO) energetic material. Journal of Computational Chemistry, 2016, 37, 163-167.	3.3	24
481	Predicted Operando Polymerization at Lithium Anode via Boron Insertion. ACS Energy Letters, 2021, 6, 2320-2327.	17.4	24
482	An NMR and Quantum-Mechanical Investigation of Tetrahydrofuran Solvent Effects on the Conformational Equilibria of 1,4-Butanedioic Acid and Its Salts. Journal of the American Chemical Society, 2002, 124, 4481-4486.	13.7	23
483	Acid atalyzed Nucleophilic Aromatic Substitution: Experimental and Theoretical Exploration of a Multistep Mechanism. Chemistry - A European Journal, 2008, 14, 3954-3960.	3.3	23
484	Hypervelocity Impact Effect of Molecules from Enceladus' Plume and Titan's Upper Atmosphere on NASA's Cassini Spectrometer from Reactive Dynamics Simulation. Physical Review Letters, 2012, 109, 213201.	7.8	23
485	Synthesis of single-component metallic glasses by thermal spray of nanodroplets on amorphous substrates. Applied Physics Letters, 2012, 100, .	3.3	23
486	Structure Prediction of G Protein-Coupled Receptors and Their Ensemble of Functionally Important Conformations. Methods in Molecular Biology, 2012, 914, 237-254.	0.9	23

#	Article	IF	CITATIONS
487	Accurate non-bonded potentials based on periodic quantum mechanics calculations for use in molecular simulations of materials and systems. Journal of Chemical Physics, 2019, 151, 154111.	3.0	23
488	Reaction Mechanisms, Kinetics, and Improved Catalysts for Ammonia Synthesis from Hierarchical High Throughput Catalyst Design. Accounts of Chemical Research, 2022, 55, 1124-1134.	15.6	23
489	Efficient Monte Carlo method for free energy evaluation of polymer chains. Fluid Phase Equilibria, 1998, 144, 415-425.	2.5	22
490	Structure-based design of mutant Methanococcus jannaschii tyrosyl-tRNA synthetase for incorporation of O-methyl-L-tyrosine. Proceedings of the National Academy of Sciences of the United States of America, 2002, 99, 6579-6584.	7.1	22
491	The MSXX Force Field for the Barium Sulfateâ^'Water Interface. Journal of Physical Chemistry B, 2002, 106, 9951-9966.	2.6	22
492	Structures, Mechanisms, and Kinetics of Ammoxidation and Selective Oxidation of Propane Over the M2 Phase of MoVNbTeO Catalysts. Topics in Catalysis, 2011, 54, 659-668.	2.8	22
493	Inhibition of Hotspot Formation in Polymer Bonded Explosives Using an Interface Matching Low Density Polymer Coating at the Polymer–Explosive Interface. Journal of Physical Chemistry C, 2014, 118, 19918-19928.	3.1	22
494	Selective Enhancement of Methane Formation in Electrochemical CO <sub>2</sub> Reduction Enabled by a Raman-Inactive Oxygen-Containing Species on Cu. ACS Catalysis, 2022, 12, 6036-6046.	11.2	22
495	Spinâ€Generalized SCF Wavefunctions for H2O, OH, and O. Journal of Chemical Physics, 1970, 53, 1803-1814.	3.0	21
496	Density Functional Theory Study of the Geometry, Energetics, and Reconstruction Process of Si(111) Surfaces. Langmuir, 2005, 21, 12404-12414.	3.5	21
497	Reactive Dynamics Study of Hypergolic Bipropellants: Monomethylhydrazine and Dinitrogen Tetroxide. Journal of Physical Chemistry B, 2012, 116, 14136-14145.	2.6	21
498	ReaxFF reactive molecular dynamics on silicon pentaerythritol tetranitrate crystal validates the mechanism for the colossal sensitivity. Physical Chemistry Chemical Physics, 2014, 16, 23779-23791.	2.8	21
499	Predicted detonation properties at the Chapman–Jouguet state for proposed energetic materials (MTO) Tj ETC Chemical Physics, 2018, 20, 3953-3969.	2q1 1 0.78 2.8	84314 rgBT /( 21
500	Role of Ferryl Ion Intermediates in Fast Fenton Chemistry on Aqueous Microdroplets. Environmental Science & Technology, 2021, 55, 14370-14377.	10.0	21
501	Prediction of the Threeâ€Dimensional Structure for the Rat Urotensinâ€II Receptor, and Comparison of the Antagonist Binding Sites and Binding Selectivity between Human and Rat Receptors from Atomistic Simulations. ChemMedChem, 2010, 5, 1594-1608.	3.2	20
502	The effect of different environments on Nafion degradation: Quantum mechanics study. Journal of Membrane Science, 2013, 437, 276-285.	8.2	20
503	Predicted roles of defects on band offsets and energetics at CIGS (Cu(In,Ga)Se2/CdS) solar cell interfaces and implications for improving performance. Journal of Chemical Physics, 2014, 141, 094701.	3.0	20
504	Optimizing the oxygen evolution reaction for electrochemical water oxidation by tuning solvent properties. Nanoscale, 2015, 7, 4514-4521.	5.6	20

#	Article	IF	CITATIONS
505	First-Principles Study of Iron Oxide Polytypes: Comparison of GGA+ <i>U</i> and Hybrid Functional Method. Journal of Physical Chemistry C, 2015, 119, 556-562.	3.1	20
506	First-Order Phase Transition in Liquid Ag to the Heterogeneous G-Phase. Journal of Physical Chemistry Letters, 2020, 11, 632-645.	4.6	20
507	Graphitization of low-density amorphous carbon for electrocatalysis electrodes from ReaxFF reactive dynamics. Carbon, 2021, 183, 940-947.	10.3	20
508	Orbital Description and Properties of the BH Molecule. Journal of Chemical Physics, 1972, 57, 5296-5310.	3.0	19
509	Solvent Effects on the Secondary Structures of Proteins. Journal of Physical Chemistry A, 2000, 104, 2498-2503.	2.5	19
510	Ab-initio studies of pressure induced phase transitions in BaO. Journal of Computer-Aided Materials Design, 2001, 8, 193-202.	0.7	19
511	Dynamic Charge Equilibration-Morse stretch force field: Application to energetics of pure silica zeolites. Journal of Computational Chemistry, 2002, 23, 1507-1514.	3.3	19
512	Initial Steps in Forming the Electrode–Electrolyte Interface: H2O Adsorption and Complex Formation on the Ag(111) Surface from Combining Quantum Mechanics Calculations and Ambient Pressure X-ray Photoelectron Spectroscopy. Journal of the American Chemical Society, 2019, 141, 6946-6954.	13.7	19
513	Synergy between a Silver–Copper Surface Alloy Composition and Carbon Dioxide Adsorption and Activation. ACS Applied Materials & Interfaces, 2020, 12, 25374-25382.	8.0	19
514	Theoretical studies of the oxidized and reduced states of a model for the active site of rubredoxin. Journal of the American Chemical Society, 1977, 99, 3505-3507.	13.7	18
515	Quantum Mechanical–Rapid Prototyping Applied to Methane Activation. Topics in Catalysis, 2003, 23, 81-98.	2.8	18
516	Lancifodilactone G: Insights about an Unusually Stable Enol. Journal of Organic Chemistry, 2008, 73, 6853-6856.	3.2	18
517	Quantum mechanics based force field for carbon (QMFF-Cx) validated to reproduce the mechanical and thermodynamics properties of graphite. Journal of Chemical Physics, 2010, 133, 134114.	3.0	18
518	Composition Dependence of Glass Forming Propensity in Alâ^'Ni Alloys. Journal of Physical Chemistry C, 2011, 115, 2320-2331.	3.1	18
519	Electronic Structures of Group 9 Metallocorroles with Axial Ammines. Inorganic Chemistry, 2011, 50, 764-770.	4.0	18
520	Thermodynamics of Water Stabilization of Carboxybetaine Hydrogels from Molecular Dynamics Simulations. Journal of Physical Chemistry Letters, 2011, 2, 1757-1760.	4.6	18
521	Activation and Oxidation of Mesitylene C–H Bonds by (Phebox)Iridium(III) Complexes. Organometallics, 2015, 34, 2879-2888.	2.3	18
522	An NMR and Quantum Mechanical Investigation of Solvent Effects on Conformational Equilibria of Butanedinitrile. Journal of the American Chemical Society, 2002, 124, 9318-9322.	13.7	17

#	Article	IF	CITATIONS
523	Role of Specific Cations and Water Entropy on the Stability of Branched DNA Motif Structures. Journal of Physical Chemistry B, 2012, 116, 12159-12167.	2.6	17
524	Scaled Effective Solvent Method for Predicting the Equilibrium Ensemble of Structures with Analysis of Thermodynamic Properties of Amorphous Polyethylene Glycol–Water Mixtures. Journal of Physical Chemistry B, 2013, 117, 916-927.	2.6	17
525	Equilibrium 2H/1H fractionation in organic molecules: III. Cyclic ketones and hydrocarbons. Geochimica Et Cosmochimica Acta, 2013, 107, 82-95.	3.9	17
526	Cubic Nonlinearity Driven Up-Conversion in High-Field Plasmonic Hot Carrier Systems. Journal of Physical Chemistry C, 2016, 120, 21056-21062.	3.1	17
527	Highly Stable Organic Bisradicals Protected by Mechanical Bonds. Journal of the American Chemical Society, 2020, 142, 7190-7197.	13.7	17
528	Ab initio predictions of large hyperpolarizability push-pull polymers. Julolidinyl-n-isoxazolone and julolidinyl-n-N,N′-diethylthiobarbituric acid. Chemical Physics Letters, 1995, 242, 543-547.	2.6	16
529	Fidelity of Phenylalanyl-tRNA Synthetase in Binding the Natural Amino Acids. Journal of Physical Chemistry B, 2003, 107, 11549-11557.	2.6	16
530	Design and validation of non-metal oxo complexes for C–H activation. Chemical Communications, 2014, 50, 1748.	4.1	16
531	Highly Efficient Ni-Doped Iron Catalyst for Ammonia Synthesis from Quantum-Mechanics-Based Hierarchical High-Throughput Catalyst Screening. Journal of Physical Chemistry C, 2019, 123, 17375-17383.	3.1	16
532	Orbital Description of the Excited States of LiH. Journal of Chemical Physics, 1972, 56, 3348-3359.	3.0	15
533	Conformational analysis of aqueous pullulan oligomers: an effective computational approach. Polymer, 2002, 43, 509-516.	3.8	15
534	Chelating Base Effects in Palladium-Mediated Activation of Molecular Oxygen. Organometallics, 2012, 31, 545-552.	2.3	15
535	Analytic Derivatives of Quartic-Scaling Doubly Hybrid XYGJ-OS Functional: Theory, Implementation, and Benchmark Comparison with M06-2X and MP2 Geometries for Nonbonded Complexes. Journal of Chemical Theory and Computation, 2013, 9, 1971-1976.	5.3	15
536	Use of Ligand Steric Properties to Control the Thermodynamics and Kinetics of Oxidative Addition and Reductive Elimination with Pincer-Ligated Rh Complexes. Organometallics, 2020, 39, 1917-1933.	2.3	15
537	Theoretical studies of the geometries of O and S overlayers on the (100) surface of nickel. Solid State Communications, 1977, 23, 907-910.	1.9	14
538	Domain Motions in Phosphoglycerate Kinase using Hierarchical NEIMO Molecular Dynamics Simulations. Journal of Physical Chemistry A, 2000, 104, 2375-2383.	2.5	14
539	Prediction of the 3-D structure of rat MrgA G protein-coupled receptor and identification of its binding site. Journal of Molecular Graphics and Modelling, 2007, 26, 800-812.	2.4	14
540	Quantum chemical insights into the dissociation of nitric acid on the surface of aqueous electrolytes. International Journal of Quantum Chemistry, 2013, 113, 413-417.	2.0	14

#	Article	IF	CITATIONS
541	Predicted 3D structures of olfactory receptors with details of odorant binding to OR1G1. Journal of Computer-Aided Molecular Design, 2014, 28, 1175-1190.	2.9	14
542	Theoretical and Experimental Studies of the Dechlorination Mechanism of Carbon Tetrachloride on a Vivianite Ferrous Phosphate Surface. Journal of Physical Chemistry A, 2015, 119, 5714-5722.	2.5	14
543	Dual-Phase Mechanism for the Catalytic Conversion of <i>n</i> -Butane to Maleic Anhydride by the Vanadyl Pyrophosphate Heterogeneous Catalyst. Journal of Physical Chemistry C, 2017, 121, 24069-24076.	3.1	14
544	Extension of the Polarizable Charge Equilibration Model to Higher Oxidation States with Applications to Ge, As, Se, Br, Sn, Sb, Te, I, Pb, Bi, Po, and At Elements. Journal of Physical Chemistry A, 2018, 122, 639-645.	2.5	14
545	Dealloyed Pt2Os nanoparticles for enhanced oxygen reduction reaction in acidic electrolytes. Applied Catalysis B: Environmental, 2014, 150-151, 636-646.	20.2	13
546	Suppression of surface recombination in CuInSe2 (CIS) thin films via Trioctylphosphine Sulfide (TOP:S) surface passivation. Acta Materialia, 2016, 106, 171-181.	7.9	13
547	The 3D Structure of Human DP Prostaglandin G-Protein-Coupled Receptor Bound to Cyclopentanoindole Antagonist, Predicted Using the DuplexBiHelix Modification of the GEnSeMBLE Method. Journal of Chemical Theory and Computation, 2018, 14, 1624-1642.	5.3	13
548	DFT Mechanistic Study of Methane Mono-Esterification by Hypervalent lodine Alkane Oxidation Process. Journal of Physical Chemistry C, 2019, 123, 15674-15684.	3.1	13
549	First-Principles Molecular Dynamics in Metal-Halide Perovskites: Contrasting Generalized Gradient Approximation and Hybrid Functionals. Journal of Physical Chemistry Letters, 2021, 12, 11886-11893.	4.6	13
550	The Rydberg states of trans-1,3-5-hexatriene from ab initio and configuration interaction calculations. Chemical Physics, 1980, 53, 265-277.	1.9	12
551	Cell multipole method for molecular simulations in bulk and confined systems. Journal of Chemical Physics, 2003, 118, 5347-5355.	3.0	12
552	Thermodynamic Stability of Zimmerman Self-Assembled Dendritic Supramolecules from Atomistic Molecular Dynamics Simulations. Journal of Physical Chemistry B, 2004, 108, 10041-10052.	2.6	12
553	Synergetic Evolution of Sacrificial Bonds and Strain-Induced Defects Facilitating Large Deformation of the Bi <sub>2</sub> Te <sub>3</sub> Semiconductor. ACS Applied Energy Materials, 2020, 3, 3042-3048.	5.1	12
554	Predictions of Chemical Shifts for Reactive Intermediates in CO2 Reduction under Operando Conditions. ACS Applied Materials & amp; Interfaces, 2021, 13, 31554-31560.	8.0	12
555	Spatially projected generalized valence bond description of the pi-states of allyl radical. Theoretica Chimica Acta, 1975, 37, 253-267.	0.8	11
556	Fidelity of seryl-tRNA synthetase to binding of natural amino acids from HierDock first principles computations. Protein Engineering, Design and Selection, 2006, 19, 195-203.	2.1	11
557	Methane Activation with Rhenium Catalysts. 1. Bidentate Oxygenated Ligands. Organometallics, 2007, 26, 1505-1511.	2.3	11
558	Reactive molecular dynamics force field for the dissociation of light hydrocarbons on Ni(111). Molecular Simulation, 2008, 34, 967-972.	2.0	11

#	Article	IF	CITATIONS
559	The Transition Metal Catalyzed [π2s + π2s + σ2s + σ2s] Pericyclic Reaction: Woodward–Hoffmann Rules, Aromaticity, and Electron Flow. Journal of the American Chemical Society, 2020, 142, 19033-19039.	13.7	11
560	Spatiotemporal Temperature and Pressure in Thermoplasmonic Gold Nanosphere–Water Systems. ACS Nano, 2021, 15, 6276-6288.	14.6	11
561	THEORETICAL STUDIES OF OXYGEN BINDING. Annals of the New York Academy of Sciences, 1981, 367, 419-433.	3.8	10
562	The structure–activity relationships of methane mono-oxygenase mimics in alkane activation. Catalysis Today, 2003, 81, 263-286.	4.4	10
563	The symmetric group and the spin generalized scf method. International Journal of Quantum Chemistry, 1969, 4, 593-600.	2.0	10
564	Formation of the –N(NO)N(NO)– polymer at high pressure and stabilization at ambient conditions. Proceedings of the National Academy of Sciences of the United States of America, 2013, 110, 5321-5325.	7.1	10
565	First principles-based multiparadigm, multiscale strategy for simulating complex materials processes with applications to amorphous SiC films. Journal of Chemical Physics, 2015, 142, 174703.	3.0	10
566	Computational Design of a Pincer Phosphinito Vanadium ((OPO)V) Propane Monoxygenation Homogeneous Catalyst Based on the Reduction-Coupled Oxo Activation (ROA) Mechanism. ACS Catalysis, 2017, 7, 356-364.	11.2	10
567	Inertial dynamics of an interface with interfacial mass flux: Stability and flow fields' structure, inertial stabilization mechanism, degeneracy of Landau's solution, effect of energy fluctuations, and chemistry-induced instabilities. Physics of Fluids, 2020, 32, 082105.	4.0	10
568	Enhancing the Detonation Properties of Liquid Nitromethane by Adding Nitro-Rich Molecule Nitryl Cyanide. Journal of Physical Chemistry C, 2020, 124, 9787-9794.	3.1	10
569	Diverse Phases of Carbonaceous Materials from Stochastic Simulations. ACS Nano, 2021, 15, 6369-6385.	14.6	10
570	Intramolecular Hydrogen Bonding in Disubstituted Ethanes:Â General Considerations and Methodology in Quantum Mechanical Calculations of the Conformational Equilibria of Succinamate Monoanion. Journal of Physical Chemistry A, 2005, 109, 9083-9088.	2.5	9
571	Selectivity and specificity of substrate binding in methionyl-tRNA synthetase. Protein Science, 2009, 13, 2693-2705.	7.6	9
572	Carbonâ^'Oxygen Bond Forming Mechanisms in Rhenium Oxo-Alkyl Complexes. Organometallics, 2010, 29, 2026-2033.	2.3	9
573	First-Principles-Based Multiscale, Multiparadigm Molecular Mechanics and Dynamics Methods for Describing Complex Chemical Processes. Topics in Current Chemistry, 2011, 307, 1-42.	4.0	9
574	Thermodynamics of <i>d</i> -dimensional hard sphere fluids confined to micropores. Journal of Chemical Physics, 2011, 134, 114502.	3.0	9
575	The para-substituent effect and pH-dependence of the organometallic Baeyer–Villiger oxidation of rhenium–carbon bonds. Dalton Transactions, 2012, 41, 3758.	3.3	9
576	Large-scale Molecular Simulations of Hypervelocity Impact of Materials. Procedia Engineering, 2013, 58, 167-176.	1.2	9

#	Article	IF	CITATIONS
577	Deformation Induced Solid–Solid Phase Transitions in Gamma Boron. Chemistry of Materials, 2014, 26, 4289-4298.	6.7	9
578	Quantum Mechanical and Experimental Validation that Cyclobis(paraquatâ€ <i>p</i> â€phenylene) Forms a 1:1 Inclusion Complex with Tetrathiafulvalene. Chemistry - A European Journal, 2016, 22, 2736-2745.	3.3	9
579	Polarizable Charge Equilibration Model for Transition-Metal Elements. Journal of Physical Chemistry A, 2018, 122, 9350-9358.	2.5	9
580	Free Energy Landscape of Sodium Solvation into Graphite. Journal of Physical Chemistry C, 2018, 122, 20064-20072.	3.1	9
581	Li-diffusion at the interface between Li-metal and [Pyr14][TFSI]-ionic liquid: <i>Ab initio</i> molecular dynamics simulations. Journal of Chemical Physics, 2020, 152, 031101.	3.0	9
582	Mechanistic Studies of Styrene Production from Benzene and Ethylene Using [(η <sup>2</sup> -C <sub>2</sub> H <sub>4</sub> ) <sub>2</sub> Rh(μ-OAc)] <sub>2</sub> as Catalyst Precursor: Identification of a Bis-Rh <sup>I</sup> Mono-Cu <sup>II</sup> Complex As the Catalyst. ACS Catalysis, 2021, 11, 5688-5702.	11.2	9
583	Manganese Catalyzed Partial Oxidation of Light Alkanes. ACS Catalysis, 2022, 12, 5356-5370.	11.2	9
584	Sodium Diffusion through Aluminum-Doped Zeolite BEA System: Effect of Water Solvation. Journal of Physical Chemistry C, 2009, 113, 819-826.	3.1	8
585	Hedgehog proteins create a dynamic cholesterol interface. PLoS ONE, 2021, 16, e0246814.	2.5	8
586	Synergic Effects in the Activation of the Sweet Receptor GPCR Heterodimer for Various Sweeteners Predicted Using Molecular Metadynamics Simulations. Journal of Agricultural and Food Chemistry, 2021, 69, 12250-12261.	5.2	8
587	Immobilization of "Capping Arene―Cobalt(II) Complexes on Ordered Mesoporous Carbon for Electrocatalytic Water Oxidation. ACS Catalysis, 2021, 11, 15068-15082.	11.2	8
588	The valence bond Aufbau principle for molecular excited states. Chemical Physics Letters, 1972, 16, 157-163.	2.6	7
589	Kinks in the a/2ã€^111〉 screw dislocation in Ta. Journal of Computer-Aided Materials Design, 2001, 8, 117-12	5.0.7	7
590	The mechanism for catalytic hydrosilylation by bis(imino)pyridine iron olefin complexes supported by broken symmetry density functional theory. Dalton Transactions, 2017, 46, 12507-12515.	3.3	7
591	First principles-based multiscale atomistic methods for input into first principles nonequilibrium transport across interfaces. Proceedings of the National Academy of Sciences of the United States of America, 2019, 116, 18193-18201.	7.1	7
592	Anomalies in Supercooled Water at â^1⁄4230 K Arise from a 1D Polymer to 2D Network Topological Transformation. Journal of Physical Chemistry Letters, 2019, 10, 6267-6273.	4.6	7
593	Crack propagation in a Tantalum nano-slab. Journal of Computer-Aided Materials Design, 2001, 8, 151-159.	0.7	6
594	The Computational Materials Design Facility (CMDF): A powerful framework for multi-paradigm multi-scale simulations. Materials Research Society Symposia Proceedings, 2005, 894, 1.	0.1	6

#	Article	IF	CITATIONS
595	Rigidityâ^'Stability Relationship in Interlocked Model Complexes Containing Phenylene-Ethynylene-Based Disubstituted Naphthalene and Benzene. Crystal Growth and Design, 2009, 9, 2300-2309.	3.0	6
596	Surface and Electronic Properties of Hydrogen Terminated Si [001] Nanowires. Journal of Physical Chemistry C, 2011, 115, 12586-12591.	3.1	6
597	Predicted Ligands for the Human Urotensinâ€II Gâ€Proteinâ€Coupled Receptor with Some Experimental Validation. ChemMedChem, 2014, 9, 1732-1743.	3.2	6
598	The relation of mechanical properties and local structures in bulk Mg 54 (Cu 1â^ x Ag x ) 35 Y 11 metallic glasses: Ab initio molecular dynamics simulations. Computational Materials Science, 2014, 92, 313-317.	3.0	6
599	Stability of NNO and NPO Nanotube Crystals. Journal of Physical Chemistry Letters, 2014, 5, 485-489.	4.6	6
600	The PX Motif of DNA Binds Specifically to <i>Escherichia coli</i> DNA Polymerase I. Biochemistry, 2019, 58, 575-581.	2.5	6
601	Discovery of Dramatically Improved Ammonia Synthesis Catalysts through Hierarchical High-Throughput Catalyst Screening of the Fe(211) Surface. Chemistry of Materials, 2020, 32, 9914-9924.	6.7	6
602	Reduction of N <sub>2</sub> to Ammonia by Phosphate Molten Salt and Li Electrode: Proof of Concept Using Quantum Mechanics. Journal of Physical Chemistry Letters, 2021, 12, 1696-1701.	4.6	6
603	Operando Electrochemical Spectroscopy for CO on Cu(100) at pH 1 to 13: Validation of Grand Canonical Potential Predictions. ACS Catalysis, 2021, 11, 3173-3181.	11.2	6
604	Predicted Structure of Fully Activated Tas1R3/1R3′ Homodimer Bound to G Protein and Natural Sugars: Structural Insights into G Protein Activation by a Class C Sweet Taste Homodimer with Natural Sugars. Journal of the American Chemical Society, 2021, 143, 16824-16838.	13.7	6
605	Biased β-Agonists Favoring Gs over β-Arrestin for Individualized Treatment of Obstructive Lung Disease. Journal of Personalized Medicine, 2022, 12, 331.	2.5	6
606	Coupling of Raman Radial Breathing Modes in Double-Wall Carbon Nanotubes and Bundles of Nanotubes. Journal of Physical Chemistry B, 2009, 113, 7199-7204.	2.6	5
607	Homology modeling and molecular docking studies of Drosophila and Aedes sex peptide receptors. Journal of Molecular Graphics and Modelling, 2016, 66, 115-122.	2.4	5
608	Discovery of Novel Biased Opioid Receptor Ligands through Structureâ€Based Pharmacophore Virtual Screening and Experiment. ChemMedChem, 2019, 14, 1783-1794.	3.2	5
609	Scalable Reactive Molecular Dynamics Simulations for Computational Synthesis. Computing in Science and Engineering, 2019, 21, 64-75.	1.2	5
610	Entropic Stabilization of Water at Graphitic Interfaces. Journal of Physical Chemistry Letters, 2021, 12, 9162-9168.	4.6	5
611	THEORETICAL STUDIES OF THE BONDING OF O2 TO HEMOGLOBIN; IMPLICATIONS FOR COOPERATIVITY. , 1979, , 87-123.		4
612	Formation of water at a Pt(111) surface: A study using the reactive force field (ReaxFF). Materials Research Society Symposia Proceedings, 2005, 900, 1.	0.1	4

#	Article	IF	CITATIONS
613	Molecular Modeling of Carbohydrates with No Charges, No Hydrogen Bonds, and No Atoms. ACS Symposium Series, 2006, , 271-284.	0.5	4
614	The Predicted Binding Site and Dynamics of Peptide Inhibitors to the Methuselah GPCR from Drosophila melanogaster. Biochemistry, 2008, 47, 12740-12749.	2.5	4
615	Group Vibrational Mode Assignments as a Broadly Applicable Tool for Characterizing Ionomer Membrane Structure as a Function of Degree of Hydration. Chemistry of Materials, 2020, 32, 1828-1843.	6.7	4
616	Reaction Mechanism Underlying Pd(II)-Catalyzed Oxidative Coupling of Ethylene and Benzene to Form Styrene: Identification of a Cyclic Mono-Pd <sup>II</sup> Bis-Cu <sup>II</sup> Complex as the Active Catalyst. Organometallics, 0, , .	2.3	4
617	Threshold crack speed in dynamic fracture of silicon. Materials Research Society Symposia Proceedings, 2006, 978, .	0.1	3
618	The optimum orbitals for the H2 + D⇋H + HD exchange reaction. International Journal of Quantum Chemistry, 1969, 3, 63-66.	2.0	3
619	Direct atomistic simulation of brittle-to-ductile transition in silicon single crystals. Materials Research Society Symposia Proceedings, 2010, 1272, 1.	0.1	3
620	Transport properties of imidazolium based ionic liquid electrolytes from molecular dynamics simulations. Electrochemical Science Advances, 0, , e2100007.	2.8	3
621	Focus on the deformation mechanism at the interfacial layer in nano-reinforced polymers: A molecular dynamics study of silica - poly(methyl methacrylate) nano-composite. Mechanics of Materials, 2021, 159, 103903.	3.2	3
622	Development of the ReaxFF Reactive Force Field for Cu/Si Systems with Application to Copper Cluster Formation during Cu Diffusion Inside Silicon. Journal of Physical Chemistry C, 2021, 125, 19455-19466.	3.1	3
623	Structure, Energetics, and Spectra for the Oxygen Vacancy in Rutile: Prominence of the Ti–H <sub>O</sub> –Ti Bond. Journal of Physical Chemistry Letters, 2021, 12, 10175-10181.	4.6	3
624	Reaction Mechanism and Energetics of Decomposition of Tetrakis(1,3-dimethyltetrazol-5-imidoperchloratomanganese(II)) from Quantum-Mechanics-based Reactive Dynamics. Journal of the American Chemical Society, 2021, 143, 16960-16975.	13.7	3
625	Order-Tuned Deformability of Bismuth Telluride Semiconductors: An Energy-Dissipation Strategy for Large Fracture Strain. ACS Applied Materials & Interfaces, 2021, 13, 57629-57637.	8.0	3
626	Complete inhibition of a polyol nucleation by a micromolar biopolymer additive. Cell Reports Physical Science, 2022, 3, 100723.	5.6	3
627	Recent Advances in Simulation of Dendritic Polymers. Materials Research Society Symposia Proceedings, 1998, 543, 299.	0.1	2
628	Molecular Dynamics Simulations of Supercooled Liquid Metals and Glasses. Materials Research Society Symposia Proceedings, 2000, 644, 231.	0.1	2
629	MPiSIM: Massively parallel simulation tool for metallic system. Journal of Computer-Aided Materials Design, 2001, 8, 185-192.	0.7	2
630	London Dispersion Corrections to Density Functional Theory for Transition Metals Based on Fitting to Experimental Temperature-Programmed Desorption of Benzene Monolayers. Journal of Physical Chemistry Letters, 2021, 12, 73-79.	4.6	2

#	Article	IF	CITATIONS
631	Experimental and Theoretical Comparison of Potential-dependent Methylation on Chemically Exfoliated WS <sub>2</sub> and MoS <sub>2</sub> . ACS Applied Materials & Interfaces, 2022, 14, 9744-9753.	8.0	2
632	SINGLET MOLECULAR OXYGEN CHEMISTRY AND IMPLICATIONS FOR FLAVIN-COFACTOR HYDROXYLATIONS. , 1979, , 513-555.		1
633	First principles multiscale modeling of physico-chemical aspects of tribology. Tribology Series, 2001, , 15-33.	0.1	1
634	Multi-paradigm multi-scale modeling of dynamical crack propagation in silicon using the ReaxFF reactive force field. Materials Research Society Symposia Proceedings, 2005, 904, 1.	0.1	1
635	Quantization of crack speeds in dynamic fracture of silicon: Multiparadigm ReaxFF modeling. Materials Research Society Symposia Proceedings, 2006, 910, 7.	0.1	1
636	Prediction of the Size Distributions of Methanolâ^²Ethanol Clusters Detected in VUV Laser/Time-of-Flight Mass Spectrometry. Journal of Physical Chemistry A, 2009, 113, 6865-6875.	2.5	1
637	New Quantum Mechanics Based Methods for Multiscale Simulations with Applications to Reaction Mechanisms for Electrocatalysis. Topics in Catalysis, 2020, 63, 1658-1666.	2.8	1
638	Electrochemical Performance and Structures of Chromium and Molybdenum-Doped ε-Li <sub><i>x</i></sub> VOPO <sub>4</sub> Predicted as Promising Cathodes for Next Generation Lithium-Ion Batteries. Journal of Physical Chemistry C, 2021, 125, 275-282.	3.1	1
639	Deformation and Failure Mechanisms of Thermoelectric Type-I Clathrate Ba <sub>8</sub> Au <sub>6</sub> Ge <sub>40</sub> . ACS Applied Materials & Interfaces, 2022, 14, 4326-4334.	8.0	1
640	Application of lightweight threading techniques to computational chemistry. Journal of Computer-Aided Materials Design, 2001, 8, 173-184.	0.7	0
641	Multiscale Multiparadigm in Silico Design of New Materials for Li-ion Batteries. ECS Meeting Abstracts, 2012, , .	0.0	0
642	Lithium Dendrite Inhibition on Post-Charge Anode Surface: The Kinetics Role. Materials Research Society Symposia Proceedings, 2015, 1774, 31-39.	0.1	0
643	Quantum mechanics based mechanisms for selective activation of hydrocarbons by mixed metal oxide heterogeneous catalysts – A tribute to Robert Grasselli. Catalysis Today, 2021, 363, 3-9.	4.4	0
644	Atomic and Molecular Unit Energy Conversion Catalysis of Carbon Dioxides in Value-Added Chemical Fuels. Springer Series in Materials Science, 2021, , 743-766.	0.6	0
645	Reactive scattering of water group ions on ice surfaces with relevance to Saturn's icy moons. Icarus, 2022, 379, 114967.	2.5	0
646	A Perspective of Materials Modeling. , 2005, , 2707-2711.		0
647	5HTR1E receptor interacts with Neurotrophic factorâ€Î±1 and serotonin to activate two distinct signaling pathways. FASEB Journal, 2022, 36, .	0.5	Ο